COOMET Key Comparison
(Bilateral)
COOMET.PR-K1.b.1
(COOMET project 653/RU/14)
Spectral Irradiance 200 nm to 350 nm
Final Report

B. Khlevnoy[1], M. Solodilov[1], P. Sperfeld[2] and S. Pape[2]

[1] *All-Russian Research Institute for Optical and Physical Measurement (VNIIOFI), Moscow, Russia*
[2] *Physikalisch-Technische Bundesanstalt (PTB), Braunschweig, Germany*

Moscow, 2019

Abstract

A bilateral comparison of the spectral irradiance in wavelengths range from 200 nm to 350 nm was carried out between VNIIOFI (Russia) and PTB (Germany) using 30W deuterium lamps as artefacts. The purpose of the comparison is to provide VNIIOFI a link to the results of the key comparison **CCPR-K1.b**. PTB was a link laboratory, but VNIIOFI served as a pilot. The degree of equivalence (DoE) of VNIIOFI, i.e. the difference of spectral irradiance values measured by VNIIOFI from the key comparison reference value (KCRV), varied from -2.5 % to 1.6 % and was within the standard uncertainty.

Contents

1 Introduction

At its meeting in March 1997, the Consultative Committee for Photometry and Radiometry, CCPR, identified several key comparisons in the field of optical radiation metrology. In particular, it decided that a key comparison of spectral irradiance in the air-UV spectral range shall be carried out. The comparison "CCPR-K1.b Spectral Irradiance 200 nm to 350 nm" was started in 2003 and completed in 2008 [1]. It was piloted by the Physikalisch-Technische Bundesanstalt (PTB), Germany.

All-Russian Research Institute for Optical and Physical Measurements (VNIIOFI) did not take part in CCPR-K1.b. VNIIOFI and PTB agreed to conduct a bilateral comparison that allowed to determine the Degrees of Equivalence (DoE) of VNIIOFI, i.e. the relative difference of VNIIOFI measurement result to the Key Comparison Reference Value (KCRV), which were defined in CCPR-K1.b.

This bilateral comparison was carried out within the RMO Euro-Asian Cooperation of National Metrological Institutions (COOMET); the identification of the COOMET project was 653/RU/14. This RMO comparison was registered at KCDB as COOMET.PR-K1b.1.

The technical protocol of this RMO comparison was made as close as possible to the technical protocol used for CCPR-K1.b. Three 30 W deuterium lamps were used as traveling artifacts.

The comparison was carried out and its results were analysed in accordance with three CCPR Guidelines: Guidelines for CCPR and RMO Bilateral Key Comparisons (CCPR-G5) [2], Guidelines for RMO PR Key Comparisons (CCPR-G6) [3] and Guidelines for CCPR Key Comparison Report Preparation (CCPR-G2) [4].

2 Organization

2.1 Participants

The participants of the COOMET.PR-K1.b.1 bilateral key comparison were VNIIOFI and PTB. The participant details are presented in Table 2.1. VNIIOFI was a laboratory, which needed to be linked to CCPR-K1.b (non-link laboratory). PTB acted as a link laboratory. PTB participated in CCPR-K1. b and provided the link of results between this bilateral KC and CCPR-K1.b.

VNIIOFI acted as the pilot laboratory and was responsible for developing the comparison protocol, preparing travelling standards, checking stability of travelling standards, registering the comparison, preparing Draft A and subsequent work.

PTB as a link laboratory was responsible for Pre-Draft A.

Table 2.1. Participant details

Laboratory	Function	Contact person	Contact
Physikalisch-Technische Bundesanstalt (PTB) 4.11 Spectroradiometry Bundesallee 100 D 38116 Braunschweig Germany	Link lab	Peter Sperfeld	Tel. +49 531 592 4144 Fax +49 531 592 69 4144 Email: Peter.Sperfeld@ptb.de
All-Russian Research Institute for Optical and Physical Measurements (VNIIOFI), Ozernaya 46, 119361 Moscow, Russia	Pilot lab Non-link lab	Boris Khlevnoy	Tel: +7 (495) 437-29-88 Fax: +7 (495) 437-29-92 Email: khlevnoy-m4@vniiofi.ru

2.2 Form of comparison

The comparison was principally carried out through the calibration of a group of three travelling sta ndard lamps (artefacts).

Following the requirements CCPR-G5 [2] (paragraphs 5.2 – 5.4) a third party (CCPR Secretary) wa s designated for the comparison, and all the measurement results, both from the non-link laboratory (VNIIOFI) and the link laboratory (PTB) were submitted electronically to the third party upon com pletion of each measurement, to ensure blindness of the comparison. At completion of all measurem ents, the third party sent all the data received to the link laboratory (PTB), which was responsible fo r Pre-Draft A process.

The comparison was carried out in the following sequence: VNIIOFI – PTB – VNIIOFI. Originally only two VNIIOFI measurements and one PTB measurement in between them were planed. Howev er, because of bad agreement between the first and second VNIIOFI measurements and a distance er ror at PTB more measurements were performed and the actual sequence was the following:

VNIIOFI #1 – PTB #1 – VNIIOFI #2 – VNIIOFI #3 – VNIIOFI #4 – PTB #2 – VNIIOFI #5

The actual timetable of measurements are shown in Table 2.2.

Table 2.2. Timetable of measurements

Activity	Date
VNIIOFI Round #1	January – February 2015
PTB Round #1	March 2015
VNIIOFI Round #2	September 2015
VNIIOFI Round #3	December 2015
VNIIOFI Round #4	August 2016
PTB Round #2	August 2016
VNIIOFI Round #5	February 2017

3. Description of artefact

The measurement artefact was a set of three travelling standard deuterium lamp systems. The lamps were 30 W deuterium lamps of the type HAMAMATSU L6308. The lamps were mounted in housing by the company “SPECTR” (Russia). Each system consists of a deuterium lamp in the housing, associated power supply and a shunt resistor (Fig. 3.1). Each lamp has to be operated with its own specific power supply and shunt resistor. Serial numbers of the lamp systems and their components are presented in Table 3.1.

Figure 3.1. Measurement artifact: deuterium lamp in housing, power supply, shunt resistor and alignment jig

An alignment jig marked with “amtlicher Jig 2” was used for all lamp systems. It has a glass window and a “cross” target in its centre (Fig. 3.2). The jig had to be connected to the internal (black) screen of the lamp housing. The lamp was aligned in such a way that the jig glass was perpendicular to an alignment laser of the spectral irradiance facility and the laser went through the target centre. The front surface of the jig glass window was used as the reference plane for the distance measurement (Fig.3.2 right).

Table 3.1. Serial numbers of lamp systems and components

Lamp Identification	Lamp Serial No.	Power Supply No.	Shunt Resistor No.
DL1	14000023-DC4799	14010023	1822
DL2	14000024-DC4802	14010024	096437
DL3	14000025-DC4800	14010025	096482

Figure 3.2. Alignment jig (right) and reference plane for the distance measurement (left)

The lamp power supply was specially designed for the 30 W deuterium lamps. Each power supply was equipped with its own shunt resistor for measuring the lamp current. More details of the lamp description can be found in the comparison protocol.

The pilot had performed pre-alignment of each lamp using the mounting inside the lamp housing in such a way that its UV-irradiance to be maximum on the optical axis defined by the housing and the jig.

The pilot had carried out an initial ageing of each lamp for approximately 200 h. During that time the lamps were switched on and off several times. The typical lamp drift after aging was 0.07 % per hour.

The artifacts were transported between participants in an aircraft cabin by members of the participating laboratories and handled by authorized persons only. No cleaning of the lamps, no housing opening was attempted during the comparison.

4. VNIIOFI measurement facility and uncertainty

4.1. Primary scale realisation

Spectral Irradiance scale in the spectral range from 200 nm to 350 nm was realised using a high-temperature blackbody of the BB3500M type. Emissivity of BB3500M was estimated to be approximately 0.9995 with standard uncertainty varied from 0.06% at 350 nm to 0.1% at 200 nm.

$$E_{\mathrm{BB}}(\lambda,T)=\frac{A}{d^2}\cdot\varepsilon_{\mathrm{eff}}\cdot\frac{c_1}{\pi\lambda^5 n^2}\cdot\frac{1}{\exp\left(\frac{c_2}{\lambda T n}\right)-1} \tag{4.1}$$

where

$c_1 = 3.741772\cdot10^{-16}$ W m^2

$c_2 = 1.438777\cdot10^{-2}$ K m

λ - wavelength in air

T – temperature of the blackbody

n – air refractive index (calculated according to [5])

$\varepsilon_{\mathrm{eff}}$ – effective emissivity of the blackbody

A – Area of the precision blackbody aperture

d – distance from the blackbody aperture to the sphere entrance aperture.

The temperature of the B3500M was approximately 3020 K. A radiation thermometer of the TSP type was used to measure the BB3500M temperature. The thermometer was calibrated against high-temperature fixed points (HTFP) Co-C (1597.4 K), Re-C (2747.8 K) and WC-C (3020.6 K). Thermodynamic temperatures of the Co-C and Re-C HTFPs were measured by means of primary radiometric methods within the international project “Implementing the new Kelvin (InK)” [6]. The WC-C temperature was found as an average of independent values obtained at four different NMIs by comparing with a copper fixed point. The standard uncertainty of the average temperature of WC-C was estimated as 0.35 K [7]. The overall standard uncertainty of BB3500M temperature was 0.7 K. The calibration of the TSP thermometer was checked against the WC-C fixed-point blackbody before each set of measurements.

In front of the BB3500M blackbody there was a precision aperture with diameter of approximately 8 mm. The temperature of the aperture holder was stabilised at the level of 20 ºC using a liquid thermostat.

4.2. Measurement facility

The lamps used as the comparison transfer standards were measured by means of direct comparison with the BB3500M blackbody using a spectral comparator based on a double monochromator.

The facility used is shown schematically in Figure 4.1. Generally, the facility is used for the spectral range from 200 nm to 2500 nm for different type of sources. For the present comparison it was used

for deuterium lamps only in the range from 200 nm to 350 nm. The facility consists of the following elements:

1. The BB3500M blackbody
2. Precision aperture
3. Lamps to be measured
4. Alignment lasers
5. TSP radiation thermometer
6. Integrating sphere
7. Monochromator
8. Detectors
9. Focusing mirror
10. Flat mirrors
11. Alignment laser
12. Set of light shields
13. Shutters

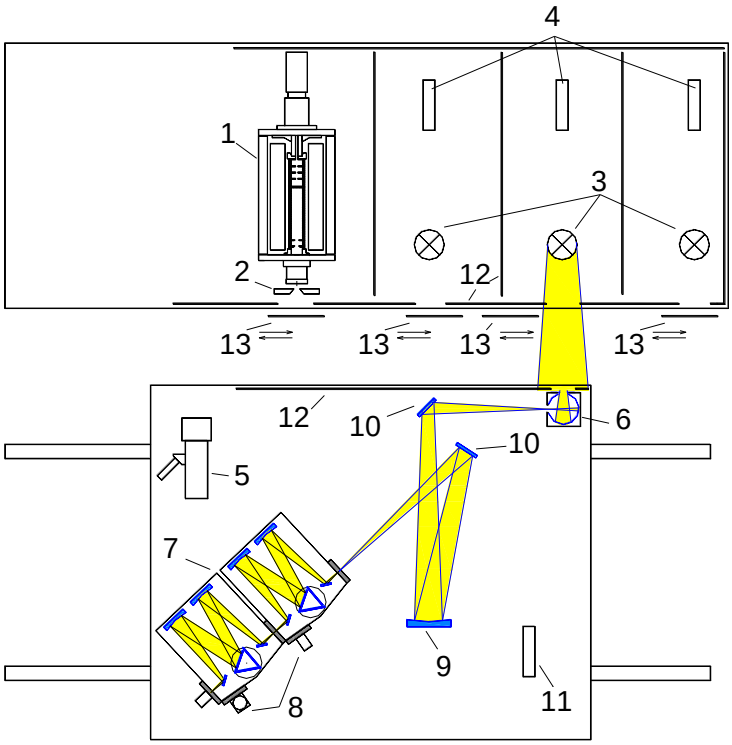

Figure 4.1. Spectral Irradiance facility of VNIIOFI

The blackbody and lamps were installed on an optical table and covered with a light tight box with holes in front of the sources equipped with shutters (13).

A spectral comparator consisted of the integrating sphere (6), monochromator (7), focusing optics (9, 10) and detectors (8) was assembled on a translation stage. The radiation thermometer (5) and the alignment laser (11) were installed on the same translation stage. The optical plate of the translation stage was covered with a light tight box with holes in front of the sphere and thermometer.

Spectral irradiance of the sources was measured in the plane of the entrance aperture of the integrating sphere. The distance from the lamps to the sphere was 400 mm, and the distance from the blackbody aperture to the sphere was approximately 470 mm. The exit aperture of the sphere was imaged to the monochromator entrance slit by the focusing mirror through the flat mirrors.

4.2.1. Integrating sphere

The integrating sphere had an internal diameter of 40 mm and was covered inside with $BaSO_4$. The sphere had two apertures located on orthogonal sides: a circular entrance aperture with diameter of 11 mm and an exit slit with the dimensions of 4×15 mm.

4.2.2. Monochromator

The monochromator used was an additive-mode double grating monochromator of the DTMc300 type (producer is Bentham Instruments Limited) with focal length of 300 mm. In the spectral range from 200 nm to 350 nm one pair of gratings was used: 1200 g/mm with dispersion of 1.35 nm/mm. Slit width used was 3 mm for both entrance and exit slits. Therefore, the spectral bandwidth was 4.05 nm.

Wavelength accuracy and wavelength repeatability of the monochromator were 0.15 nm and 0.05 nm respectively.

4.2.2.1. Bandwidth correction

Bandwidth correction was applied following analysis presented in the section 5.4.2.1 of the CCPR-K1b final report [1]. The correction factor was calculated as

$$k_{BW}(\lambda_i) = \frac{\left(S_{Lamp}(\lambda_i) + \Delta S_{Lamp}(\lambda_i)\right)/\left(S_{BB}(\lambda_i) + \Delta S_{BB}(\lambda_i)\right)}{R(\lambda_i)} \tag{4.2}$$

where $R(\lambda_i)$ is measured ratio of Lamp-to-Blackbody signals at wavelength λ_i; $\Delta S_{Lamp}(\lambda_i)$ and $\Delta S_{BB}(\lambda_i)$ are corrections to the signals of the lamp and blackbody, respectively, calculated as.

$$\Delta S(\lambda_i) = -\frac{b^2}{12}\left[\frac{S(\lambda_{i-1}) - 2S(\lambda_i) + S(\lambda_{i+1})}{(\Delta\lambda)^2}\right] \tag{4.3}$$

where b is the bandwidth and $\Delta\lambda$ – is a spectral step. In our case b was 4.05 nm and $\Delta\lambda$ =10 nm. Typical corrections are presented in Table 4.1.

4.2.3. Detectors

For the present comparison only one detector was used: room-temperature PMT of the type Hamamatsu R1527

4.2.4. Distance measurement

Distance between the lamp and the sphere, as well as between the blackbody aperture and the sphere, was measured using an extension rod type micrometer (producer is Mitutoyo). Accuracy of the micrometer is 10 μm. However, the actual uncertainty of the distance measurement was higher due a play of the mounts of the sphere, aperture and lamps.

Table 4.1. Typical correction factors due to monochromator bandwidth applied for VNIIOFI measurements

Wavelength, nm λ_i	Correction factor $k_{BW}(\lambda_i)$	Wavelength, nm λ_i	Correction factor $k_{BW}(\lambda_i)$
200	1.028	280	1.003
210	1.035	290	1.003
220	1.032	300	1.002
230	1.026	310	1.002
240	1.016	320	1.001
250	1.010	330	1.000
260	1.006	340	1.000
270	1.003	350	1.000

4.3. Measurement sequence

The comparison lamps were measured by means of direct comparison with the blackbody. The comparisons were performed wavelength-by-wavelength, i.e. the measurement sequence was as follows:

- Wavelength set
- Translation stage moved to the position where the radiation thermometer stands in front of the Blackbody
- Blackbody temperature measured and saved
- Translation stage moved to the Lamp position
- Shutter of the Lamp opened
- Detector signal read 50 to 100 times (depend on wavelength) and average value and its standard deviation saved.
- The Shutter closed, dark signal read 50 to 100 times and average value and its standard deviation saved
- Translation stage moved to the Blackbody position
- Shutter of the Blackbody opened
- Detector signal read 50 to 100 times and average value and its standard deviation saved.
- The Shutter closed, dark signal read 50 to 100 times and average value and its standard deviation saved
- Ratio (Lamp signal – lamp Dark) / (Blackbody signal – blackbody Dark) calculated and saved
- Translation stage moved to the position where the radiation thermometer stands in front of the Blackbody
- Blackbody temperature measured and saved
- Two (sometimes four) Ratios were measured for each wavelength with necessary stage movements.
- New wavelength was set and the measurement cycle repeated.

The standard deviations of the measured signals were used later for estimation of Type A uncertainties. The associated uncertainty component is identified below as "Noise/Signal".
Three to four independent measurements were done for each comparison lamp. Each independent measurement was done with independent realignment of the lamps. Standard deviation of the mean calculated from these independent measurements was used for estimation of the uncertainty component identified below as "Reproducibility".
Five Rounds of measurements were done at VNIIOFI.

4.4. Uncertainty budget

4.4.1. Uncertainty components associated with the blackbody (scale realization)

4.4.1.1. The first and second **radiation constants** c_1 and c_2 of the Planck law are known with uncertainties negligible comparing with other components. Therefore, these uncertainties were not included in the budget.

4.4.1.2. Air **refractive index** (**n**) estimation depends on a model and air conditions such as temperature, pressure, humidity. Varying these parameters, the standard uncertainty of **n** was estimated as 0.00002. The blackbody spectral irradiance uncertainty associated with n was calculated using the Planck law.

4.4.1.3. Estimation of the blackbody emissivity and its uncertainty was based on modeling using the STEEP3 software [8]. The emissivity was estimated to be approximately equal to 0.9995 with the standard uncertainty varied from 0.06% at 350 nm to 0.1% at 200 nm.

4.4.1.4. Blackbody temperature measurement uncertainty was estimated as 0.7 K. The main sources of temperature uncertainty were determination of T_{90} of the WC-C point, reproducibility of WC-C melting temperature, size-of-source effect and stability of the radiation thermometer. The blackbody spectral irradiance uncertainty associated with n was calculated using the Planck law.

4.4.1.5. Blackbody non-uniformity was estimated on the base of preliminary blackbody mapping. It corresponds to the temperature non-uniformity standard uncertainty of approximately 0.3 K. The blackbody spectral irradiance uncertainty associated with non-uniformity was calculated using the Planck law.

4.4.1.6. Blackbody instability was measured directly during the lamp calibration. The typical temperature instability standard uncertainty was not higher than 0.1 K. The blackbody spectral irradiance uncertainty associated with instability was calculated using the Planck law.

4.4.1.7. It is known [9] that radiation of a graphite blackbody suffer from absorption of carbon-based moleculars (C_2, C_3, CN) at very high temperatures. It was shown in [9] that in visible range the absorption become notable when temperature reaches 3100 K. In UV absorption has not been studied yet. Although the temperature used was 3020 K (lower than 3100 K) we assumed that absorption might happen. Therefore, we included uncertainty associated with possible absorption effect, although we have not apply any correction of spectral irradiance values related to this effect. The value of standard uncertainty varies from 0.3 % at 350 nm to 0.5 % at 200 nm.

4.4.1.8. Diameter of the blackbody aperture was 8.0226 mm. Its area was known with standard uncertainty of 0.04 %.

4.4.1.9. The last component in the blackbody budget is an uncertainty associated with distance from the blackbody aperture to the integration sphere. It was estimated as 0.05 %.

Table 4.2. Standard uncertainty components of the blackbody spectral irradiance in percentage

λ, nm	Air refractive index ***n***	Emissivity	Temperature measurement (ΔT=0.7 K)	Blackbody Uniformity (0.3K)	Blackbody Stability (0.1K)	Absorption	Aperture area	Blackbody-to-sphere Distance	**Scale** Combined (k=1), %
200	0.04	0.1	0.55	0.24	0.08	0.50	0.04	0.05	**0.80**
210	0.04	0.1	0.52	0.22	0.08	0.50	0.04	0.05	**0.77**
220	0.03	0.1	0.50	0.21	0.07	0.50	0.04	0.05	**0.75**
230	0.03	0.1	0.48	0.21	0.07	0.50	0.04	0.05	**0.74**
240	0.03	0.1	0.46	0.20	0.07	0.50	0.04	0.05	**0.72**
250	0.03	0.1	0.44	0.19	0.06	0.40	0.04	0.05	**0.64**
260	0.03	0.08	0.43	0.18	0.06	0.40	0.04	0.05	**0.62**
270	0.03	0.08	0.41	0.18	0.06	0.40	0.04	0.05	**0.61**
280	0.03	0.08	0.39	0.17	0.06	0.40	0.04	0.05	**0.60**
290	0.02	0.08	0.38	0.17	0.05	0.40	0.04	0.05	**0.59**
300	0.02	0.08	0.37	0.16	0.05	0.30	0.04	0.05	**0.52**
310	0.02	0.06	0.36	0.15	0.05	0.30	0.04	0.05	**0.50**
320	0.02	0.06	0.35	0.15	0.05	0.30	0.04	0.05	**0.49**
330	0.02	0.06	0.34	0.15	0.05	0.30	0.04	0.05	**0.48**
340	0.02	0.06	0.33	0.14	0.05	0.30	0.04	0.05	**0.48**
350	0.02	0.06	0.32	0.14	0.05	0.30	0.04	0.05	**0.47**

4.4.2. Uncertainty components associated with lamp calibration

4.4.2.1. Distance. Standard uncertainty associated with measurement of distance between a lamp and the sphere is 0.05 %. *Systematic effect*.

4.4.2.2. Bandwidth. Standard uncertainty associated with the bandwidth correction was estimated as

$$u_{BW} = (k_{BW}(\lambda_i) - 1)/2/\sqrt{3} \tag{4.4}$$

where $k_{BW}(\lambda_i)$ is the bandwidth correction factor (see equation 3.2). *Systematic effect*.

4.4.2.3. Wavelength accuracy of the monochromator Δλ is better than 0.15 nm. Corresponding lamp spectral irradiance standard uncertainty was calculated as

$$u_{wa} = \frac{dR(\lambda)}{d\lambda} \cdot \Delta\lambda / \sqrt{3} \tag{4.5}$$

where $dR(\lambda)$ is the lamp-to-blackbody ratio measured with the spectral comparator. *Systematic effect*.

4.4.2.4. Wavelength repeatability, according to the monochromator producer, is 0.05 nm. Corresponding uncertainty was evaluated similar to 1.4.3. *Random effect*.

4.4.2.5. Type A uncertainty components

4.4.2.5.1. Noise/signal. Noise/signal uncertainty included standard deviations of the lamp, blackbody and dark signals, and discrepancy of two ratios measured at the same wavelength:

$$u_{noise} = \sqrt{\frac{\left(\sigma_{lamp}^2 + \sigma_{l,dark}^2\right)/S_{lamp}^2 + \left(\sigma_{BB}^2 + \sigma_{BB,dark}^2\right)/S_{BB}^2}{2N} + \frac{\left(R_1 - R_2\right)^2}{12}} \quad (4.6)$$

where σ_{lamp}, σ_{BB}, $\sigma_{l,dark}$ and $\sigma_{BB,dark}$ are standard deviations of the lamp, blackbody and dark signals, readings, respectively; S_{lamp} and S_{BB} are the average signals of the lamp and blackbody; and R_1 and R_2 are two measured Lamp/Blackbody ratios at the same wavelength. *N* is number of readings of each signal. Usually *N* was 50 or 100. Typical values of u_{noise} varied from 0.2 % at 350 nm to 2.2 % at 200 nm.

4.4.2.5.2. Reproducibility. Within each round three to four independent measurements (with independent alignment of the lamp) measurements were done. Standard deviation of the mean of these independent measurements was used as uncertainty $u_{rep,round}$ associated with reproducibility of independent measurements within one round.

Total type A uncertainty associated with one round u_A was calculated as

$$u_A = \sqrt{\frac{u_{noise}^2}{m} + u_{rep,round}^2} \quad (4.7)$$

where *m* is a number of independent measurements with a set.

4.4.2.6. Discrepancy between rounds. The differences between the average values of spectral irradiance measured in difference rounds were rather high and could not be explained by the random effects described above: wavelength repeatability, noise and reproducibility of measurements within a round. Unfortunately, we could not find the reason of the discrepancy. Therefore, we add an uncorrelated (random) component $u_{disc,rounds}$ estimated from standard deviations of the results got in different rounds. This component was estimated for two groups of rounds. The first group consists of rounds #1 (January-February 2015), #2 (September 2015) and #3 (December 2015). The second group includes rounds #3, #4 (July-August 2016) and #5 (February 2017).

The overall uncertainty budget for the lamp spectral irradiance measurement is therefore splitted into two parts: Table 4.3 presents uncertainties for the measurement rounds #1 to #3 and Table 4.4 - for the rounds #3 to #5 which is relevant for the comparison.

Table 4.3. Lamp spectral irradiance measurement uncertainty budget for round #1 to #3. All components are standard uncertainties in percentage.

λ, nm	Scale (Black body)	Distance	Band width	Wavelength accuracy	Wavelength repeatability	Discrepancy between rounds	Type A	Correlated	Uncorrelated	Combined standard uncertainty	Expanded uncertainty (*k*=2)
	correlated				uncorrelated						
200	0.80	0.05	0.80	0.90	0.30	9.0	1.4	1.39	9.0	**9.15**	**18.30**
210	0.77	0.05	0.70	0.85	0.28	2.5	1.1	1.34	2.6	**2.92**	**5.83**
220	0.75	0.05	0.60	0.85	0.28	2.2	1.3	1.33	2.3	**2.69**	**5.37**
230	0.74	0.05	0.50	0.80	0.26	2.4	0.7	1.24	2.4	**2.74**	**5.49**
240	0.72	0.05	0.20	0.75	0.24	2.4	0.6	1.12	2.4	**2.68**	**5.35**
250	0.64	0.05	0.20	0.70	0.23	2.4	0.4	0.97	2.4	**2.61**	**5.22**
260	0.62	0.05	0.10	0.65	0.21	2.2	0.4	0.91	2.2	**2.40**	**4.80**
270	0.61	0.05	0.10	0.60	0.20	2.1	0.4	0.86	2.1	**2.29**	**4.58**
280	0.60	0.05	0.00	0.55	0.19	2.0	0.4	0.82	2.0	**2.18**	**4.36**
290	0.59	0.05	0.00	0.50	0.17	1.9	0.4	0.78	1.9	**2.07**	**4.14**
300	0.52	0.05	0.0	0.50	0.16	1.9	0.4	0.72	1.9	**2.05**	**4.10**
310	0.50	0.05	0.0	0.45	0.15	1.7	0.4	0.68	1.7	**1.85**	**3.70**
320	0.49	0.05	0.0	0.40	0.14	1.7	0.4	0.64	1.7	**1.83**	**3.67**
330	0.48	0.05	0.0	0.35	0.12	1.6	0.4	0.60	1.6	**1.73**	**3.45**
340	0.48	0.05	0.0	0.35	0.12	1.4	0.4	0.59	1.4	**1.54**	**3.08**
350	0.47	0.05	0.0	0.30	0.11	1.4	0.4	0.56	1.4	**1.53**	**3.05**

Table 4.4 . Lamp spectral irradiance measurement uncertainty budget for round #3 to #5. All components are standard uncertainties in percentage.

λ, nm	Scale (Black body)	Distance	Band width	Wavelength accuracy	Wavelength repeatability	Discrepancy between rounds	Type A	Correlated	Uncorrelated	Combined standard uncertainty	Expanded uncertainty (*k*=2)
	correlated				uncorrelated						
200	0.80	0.05	0.8	0.90	0.30	3.0	1.53	1.44	3.1	**3.46**	**6.91**
210	0.77	0.05	0.7	0.85	0.28	2.0	1.32	1.34	2.2	**2.54**	**5.09**
220	0.75	0.05	0.6	0.85	0.28	1.7	1.29	1.28	1.9	**2.27**	**4.55**
230	0.74	0.05	0.5	0.80	0.26	1.4	0.60	1.20	1.5	**1.89**	**3.79**
240	0.72	0.05	0.2	0.75	0.24	1.2	0.44	1.06	1.2	**1.64**	**3.28**
250	0.64	0.05	0.2	0.70	0.23	1.0	0.39	0.97	1.1	**1.43**	**2.86**
260	0.62	0.05	0.1	0.65	0.21	0.9	0.32	0.91	0.9	**1.31**	**2.62**
270	0.61	0.05	0.1	0.60	0.20	0.9	0.31	0.86	0.9	**1.28**	**2.55**
280	0.60	0.05	0.0	0.55	0.19	0.9	0.31	0.82	0.9	**1.24**	**2.48**
290	0.59	0.05	0.0	0.50	0.17	0.9	0.31	0.77	0.9	**1.21**	**2.42**
300	0.52	0.05	0.0	0.50	0.16	0.8	0.31	0.72	0.8	**1.10**	**2.20**
310	0.50	0.05	0.0	0.45	0.15	0.8	0.21	0.68	0.8	**1.06**	**2.13**
320	0.49	0.05	0.0	0.40	0.14	0.8	0.21	0.64	0.8	**1.04**	**2.08**
330	0.48	0.05	0.0	0.35	0.12	0.8	0.21	0.60	0.8	**1.01**	**2.03**
340	0.48	0.05	0.0	0.35	0.12	0.8	0.26	0.59	0.8	**1.01**	**2.03**
350	0.47	0.05	0.0	0.30	0.11	0.8	0.26	0.56	0.8	**0.99**	**1.99**

5. PTB measurement facility and uncertainty

5.1. Description of the measurement facility and primary scale

5.1.1. Primary scale realization

The spectral irradiance scale at the Physikalisch-Technische Bundesanstalt (PTB) in Braunschweig is realized, maintained and disseminated [10] using a high temperature black-body radiator of type BB3200pg [11]. The various radiometric parameters of this black body have been characterized in detail including modifications to improve performance as well as operating and safety conditions and it is used as a primary standard of spectral irradiance [12-14].

The main parameter of a black-body, the temperature, has to be determined very accurately. At the PTB in Braunschweig, broadband-filter detectors are well established for the detector-based determination of the so-called radiometric temperature [12]. Improvements of this procedure and comparisons with other methods have been carried out and published [14-16].

For the intercomparison the black-body has been used at different distances around 750 mm and at different temperatures between 2990 K and 3060 K. The aperture with a size of 111,38 ± 0,04 mm² was used to define the source area of the black-body. The spectral irradiance at the reference plane of the spectroradiometer was then calculated according to Planck's law using the geometric parameters and the measured radiometric temperatures of the black-body.

5.1.2. Measurement facility

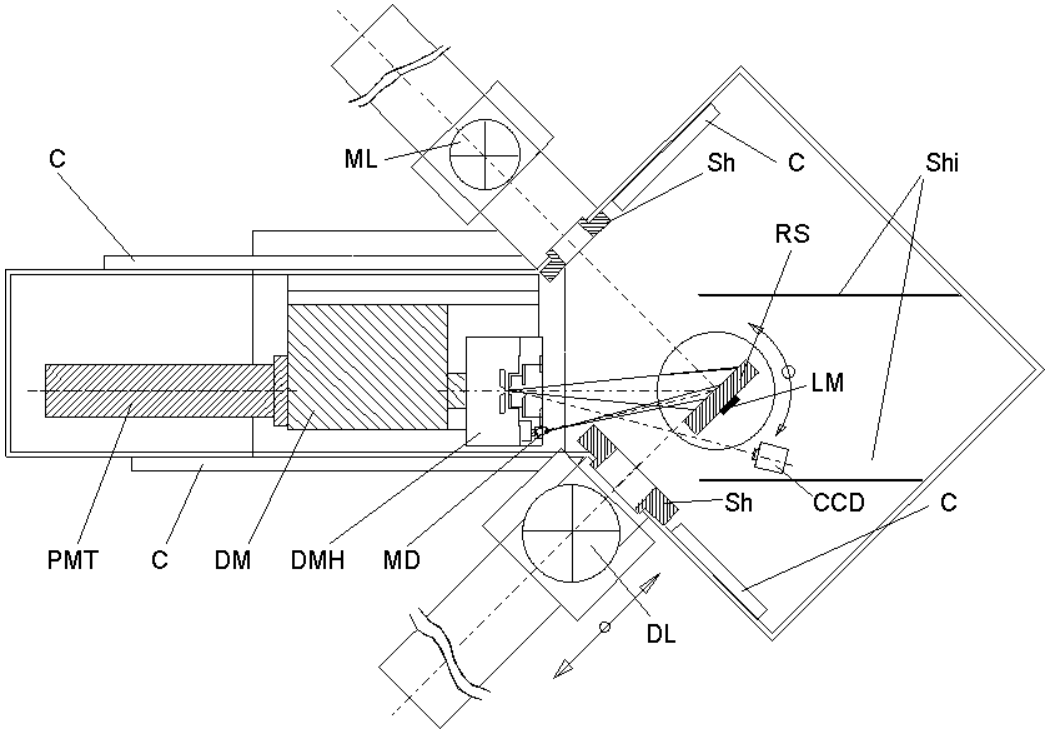

Figure 4. Spectroradiometer facility for spectral irradiance measurements optimized for air UV (top view). DM: double monochromator, PMT: solar-blind photomultiplier, RS: reflectance standard (integrating sphere), DL: deuterium lamp, ML: monitor lamp, MD: monitor photodiode, DMH: double monochromator entrance head, Sh: shutter, CCD: CCD camera, LM: laser with vertical axis plus 45° mirror for alignment, Shi: radiation shields. The reflectance standard RS is rotary. Its position shows the situation of the radiation measurement from the monitor lamp ML.

The PTB's spectroradiometer for spectral irradiance calibrations consists of an integrating sphere standard as entrance optics, for a McPherson 275D double monochromator with single gratings and a photomultiplier-tube (PMT) to cover the spectral range from 200 nm to 400 nm. The acceptance angle of the reflectance standard is limited by a precise aperture. This aperture defines the reference plane for spectral irradiance measurements. The monochromator system has a focal length of 275 mm and a numerical aperture of f / 3.5. The monochromator gratings (1200 l/mm, size 50 mm x 50 mm) are blazed for 270 nm. All three slits are operated automatically from 0 to 2.5 mm slit width by using small DC-motors with encoders. The slit heights can be varied stepwise from 2 mm to 20 mm. The photomultiplier PMT is a Hamamatsu type R7459 with a spectral sensitivity range from 180 nm to 650 nm.

The reflectance standard is an integrating sphere coated with $BaSO_4$. It is 60 mm in diameter with an opening of appr. 10 mm in diameter.

5.1.3. Calibration procedure

The black-body, working standards, or the lamps under test, were measured in the same optical path of the system in different successive measurement cycles covering each the whole recommended wavelength range. The stability of the system is verified using a deuterium monitor lamp (ML) during each measurement cycle. The signal of the black-body source, the standard lamp, or the test lamp is compared with the signal of the monitor lamp at each wavelength position by opening two different apertures and rotating the reflection standard. The monitor lamp is a photo-current stabilized 30 W deuterium lamp similar to the lamp systems used for the CCPR-K1.b comparison. Its stability is known to be better than $1 \cdot 10^{-3}\,h^{-1}$ in the UV spectral region and is frequently verified with self-consistency checks using different blackbody-calibrations.

During the intercomparison two measurement campaigns were carried out to calibrate the PTB deuterium lamp systems (DLS). The standards for the CCPR-K1.b intercomparison have been measured at least three times embedded by black-body measurements. The spectral irradiance used was averaged over the black-body calibrations for each measuring round.

5.1.4. Measurement cycle

All measurements were carried out following the same measurement procedure. The measurement started at the upper wavelength limit and at each wavelength the listed steps were carried out:

1. Go to wavelength and set according slit width
2. Turn reflection standard to test lamp and open shutter
3. Take 9 readings of photocurrent of test lamp
4. Close shutter and measure dark current
   (When operating the black body, measure temperature)
5. Turn reflection standard to monitor lamp and open shutter
6. Take 9 readings of photocurrent of monitor lamp
7. Close shutter
8. Start with step 1 at the next wavelength

5.2. Measurement uncertainties

In this document the mathematical functions and the input quantities as well as their associated uncertainties are presented. Due to its complexity, the derivation and detailed description of all components of the mathematical models is not completely described in this document.

The complete measurement uncertainty budgets for the blackbody temperature measurement, the spectral irradiance realization and the calibration procedure are described in detail in [14] and in the PTB quality-management system in documents QM-AA-4.11-01 and QM-AA-4.11-03.

5.2.1. Black-body radiator temperature measurements

The broadband-filter detectors measure the irradiance of the black-body radiator weighted according to their spectral responsivity. Their photosignal is a measure for the temperature of the black-body radiator.

This relationship can be described as follows

$$U_{\mathrm{FD}}(T_{\mathrm{BB}}) = \varepsilon \cdot (V_{\mathrm{iU}} + \delta V_{\mathrm{iU}}) \cdot \cos\varepsilon_1 \cdot \cos\varepsilon_2 \cdot \frac{A_{\mathrm{BB}} + \delta A_{\mathrm{BB}}}{d_{\mathrm{FD}}^{\,2}} \cdot (s_{\mathrm{abs}} + \delta s_{\mathrm{abs}}) \int s_{\mathrm{rel}}(\lambda) \frac{c_1}{n^2 \pi \lambda^5} \frac{1}{\exp\left(\frac{c_2}{n \cdot \lambda \cdot T_{\mathrm{BB}}}\right) - 1} \mathrm{d}\lambda \tag{5.1}$$

The quantities used in this equation are

- U_{FD} photosignal of the broadband-filter detector measured in Volts
- ε effective emissivity of the black-body radiator
- V_{iU}, δV_{iU} gain of the electrical measurements and its drift
- $\cos\varepsilon_1$, $\cos\varepsilon_2$ misalignment of filter detector to the optical axis of the black body
- A_{BB}, δA_{BB} size of the black-body opening aperture and its drift
- d_{FD} distance of the filter detector to the black-body aperture
- s_{abs}, δs_{abs} absolute spectral responsivity of the filter detector and its drift
- s_{rel} relative spectral responsivity distribution of the filter detector
- λ wavelength used for calculation
- T_{BB} radiometric temperature of the black-body radiator
- c_1,c_2 Planck contants
- n Refractive index of air

Table 5.1 Standard measurement uncertainties for blackbody radiator temperature measurements

Quantity		Type A Uncertainty	Type B Uncertainty	Uncertainty of Temperature / K @ 3150 K
effective black-body emissivity	ε		0.01 %	0.04
black-body alignment	$\cos \varepsilon_1$		1 °	0.06
detector alignment	$\cos \varepsilon_2$		1 °	0.06
black-body aperture	A_{BB}		3 µm	0.30
aperture contamination during operation	A_{BB}		0.06 %	0.14
distance detector to black-body	d_{FD}		0.05 mm	0.10
absolute detector responsivity	s_{abs}		0.1 %	0.39
relative detector responsivity	s_{rel}		0.01 %	0.04
responsivity drift between calibrations	δs_{abs}		0.05 %	0.20
detector signal readings	U_{FD}	0.01 %		0.04
gain and drift of electrical measurements	V_{iU}, δV_{iU}		0.001 %	< 0.01
Total standard measurement uncertainty				0.57
Expanded uncertainty (k=2)				1.1

5.2.2. Primary spectral irradiance unit realization

With the temperature of the blackbody-radiator known, its spectral irradiance can directly be calculated as follows

$$E(\lambda,T_P) = \varepsilon \cdot \cos\varepsilon_{diff1} \cdot \cos\varepsilon_{diff2} \cdot \frac{A_{BB} + \delta A_{BB}}{d_{diff}^2} \cdot \frac{c_1}{n^2 \pi \lambda^5} \cdot \frac{1}{\exp\left(\frac{c_2}{n \cdot \lambda \cdot T_P}\right) - 1} + \delta E(\lambda,T) \qquad (5.2)$$

The quantities used in this equation are

- E_{BB} calculated spectral irradiance of the blackbody-radiator
- ε emissivity of the black-body radiator
- $\cos \varepsilon_{diff1}$, $\cos \varepsilon_{diff2}$ misalignment of the integrating sphere opening to the optical axis of the black body
- A_{BB}, δA_{BB} size and its drift of the black body opening aperture
- d_{diff} distance of the integrating sphere opening to the black body aperture
- λ calculated wavelength
- T_P radiometric temperature of the black-body radiator determined by the filter detectors
- δE correction for black-body temperature nonuniformity
- c_1,c_2 Planck contants
- n Refractive index of air.

The wavelength λ has no associated uncertainty because it is used as an exact calculation parameter. The emissivity ε, the size of the black body opening aperture A_{BB} and its drift δA_{BB} in the mathematical model for the spectral irradiance are strongly correlated with the same input quantities

that were used to determine the black-body radiator temperature T_{BB}. The correlation slightly reduces the associated uncertainty for the temperature T_P used to calculate the spectral irradiance.

Table 5.2 Standard measurement uncertainties for primary spectral irradiance scale realization

Quantity		Uncertainty	Uncertainty in Spectral Irradiance								
			200 nm	210 nm - 220 nm	230 nm - 240 nm	250 nm - 260 nm	270 nm - 280 nm	290 nm - 300 nm	310 nm - 320 nm	330 nm - 340 nm	350 nm
black-body alignment	$\cos \varepsilon_2$	1 °	0.02%	0.02%	0.02%	0.02%	0.02%	0.02%	0.02%	0.02%	0.02%
spectroradiometer alignment	$\cos \varepsilon_1$	1 °	0.02%	0.02%	0.02%	0.02%	0.02%	0.02%	0.02%	0.02%	0.02%
distance diffusor to black body	d_{diff}	0.05 mm	0.02%	0.02%	0.02%	0.02%	0.02%	0.02%	0.02%	0.02%	0.02%
effective black-body emissivity*	ε	0.01%	0,02%	0,02%	0,01%	0,01%	0,01%	0,01%	0,01%	0,01%	0,01%
black-body aperture (diameter)*	A_{BB}	3 µm	0,15%	0,12%	0,11%	0,09%	0,08%	0,07%	0,06%	0,05%	0,05%
aperture contamination during operation*	δA_{BB}	0.06 %	0,06%	0,05%	0,05%	0,04%	0,04%	0,03%	0,03%	0,02%	0,02%
temperature determination*	T_{P}	0.46 K	0,33%	0,30%	0,28%	0,25%	0,24%	0,22%	0,21%	0,19%	0,19%
black-body temperature nonuniformity	δE	0.15 K	0,07%	0,07%	0,06%	0,06%	0,05%	0,05%	0,05%	0,04%	0,04%
Total standard measurement uncertainty			**0,38%**	**0,34%**	**0,31%**	**0,28%**	**0,26%**	**0,24%**	**0,22%**	**0,21%**	**0,20%**

* The uncertainty values for black-body emissivity, aperture and aperture contermination are strongly correlated with the temperature determination. Therefore the uncertainty for the temperature determination is slighty reduced by these parts and the correlation is taken into account in this uncertainty budget. For details see [14].

5.2.3. Calibration procedure

The mathematical model of the calibration procedure considers that separate measurements of the monitor lamp against the working standard *B* (at the time t_1) and the transfer standard *S* (at the time t_2) have to be combined. Several correction factors κ have to be implemented under varying conditions to allow simplifications of the complex physical model and to account for variations of system parameters. The determination of the spectral irradiance of the transfer standard S can then be expressed as follows

$$E_S(\lambda,t_2,T_S) = \frac{v_S(\lambda_2,b,t_2)}{v_M(\lambda_2,b,t_2)} \cdot \kappa_{\lambda,S,M}(\lambda,\lambda_2,t_2) \cdot \kappa_{b,S,M}(\lambda,b) \cdot \kappa_{L,S,M}(t_2) \cdot \kappa_{\varepsilon,S}(t_2) \cdot \kappa_{d,S}(t_2) \cdot \frac{\kappa_{I,S}(t_2)}{\kappa_{I,M}(t_2)} \cdot \frac{1}{\kappa_{t,M}(\lambda,t_2,t_1)} \cdot$$

$$\frac{v_M(\lambda_1,b,t_1)}{v_B(\lambda_1,b,t_1)} \cdot \kappa_{\lambda,M,B}(\lambda,\lambda_1,t_1) \cdot \kappa_{b,M,B}(\lambda,b) \cdot \kappa_{L,M,B}(t_1) \cdot \frac{1}{\kappa_{\varepsilon,B}(t_1) \cdot \kappa_{d,B}(t_1)} \cdot \frac{\kappa_{I,M}(t_1)}{\kappa_{I,B}(t_1)} \cdot \frac{1}{\kappa_{t,B}(\lambda,t_1,t_0)}$$

$$\cdot E_B(\lambda,t_0) \qquad (5.3)$$

The quantities used in this equation are

- E_S calibrated spectral irradiance of the transfer standard
- t_0, t_1, t_2 times of measurements/calibrations
- λ calculated wavelength
- λ_1, λ_2 wavelengths set at the spectroradiometer at times t_1 and t_2
- b spectral bandwidth of the spectroradiometer
- v_S, v_B, v_M photosignals of the lamps
- $\kappa_{d,S}$, $\kappa_{d,B}$ correction factor for distance settings of the transfer standard and the working standard
- $\kappa_{\varepsilon,S}$, $\kappa_{\varepsilon,B}$ correction factor for alignment of the transfer standard and the working standard, also considering irradiance nonuniformities
- $\kappa_{L,S,M}$, $\kappa_{L,M,B}$ combined correction factor for nonlinearity of the measurement electronics settings at times t_1 and t_2
- $\kappa_{\lambda,S,M}$, $\kappa_{\lambda,M,B}$ combined correction factor for wavelength settings at times t_1 and t_2
- $\kappa_{b,S,M}$, $\kappa_{b,M,B}$ combined correction factor for spectroradiometer bandwidth
- $\kappa_{I,S}$, $\kappa_{I,B}$, $\kappa_{I,M}$ correction factor for electrical current settings of the lamps
- $\kappa_{t,B}$, $\kappa_{t,M}$ correction factor for the drift of the working standard and the monitor lamp / measurement facility since the last measurement or calibration
- E_B spectral irradiance of the working standard

All correction factors are selected to be one under ideal conditions of the defined calibration procedures. Their associated uncertainties are considered for these conditions.

The combined correction factors take into account, that maladjustment of a quantity (e.g. the wavelength λ) has the same effect on the monitor lamp and the other lamp measured at the same time[1].

[1] If for instance the spectral distribution of the two lamps is similar (same lamp type), a maladjustment of the wavelength has a negligible effect on the ratio of the photosignals measured at the same time.

Therefore the associated measurement uncertainty of this quantity for the spectral irradiance calibration can be significantly lower than usually assumed.

Times of measurements t_0, t_1, t_2

The parameters t_0, t_1, t_2 are the points in measurement time when the measurement were taken. t_0 is the time when the working standard has been calibrated the last time. The working standard then is measured at the time t_1 again. The difference t_1-t_0 equals the burning time of the working standard since the last calibration. When using the black-body, t_1-t_0 = 0 because the spectral irradiance is calculated instantaneously during the measurements. The time t_2 is when the transfer standard is calibrated. The difference t_2-t_1 equals the burning time of the monitorlamp since the last measurements with the working standard.

Photosignals v_S, v_B, v_M of the lamps

The photosignals of the lamps are linked to the readout of the measurement electronics. They are averaged over at least 16 readouts and substracted by the corresponding dark-signal. The photosignal v_M of the monitorlamp is taken directly after the photosignals of the standard lamp v_S or the black-body v_B have been measured. Therefore the measurements can be handled as synchronous readouts to compensate short-term instabilities of the system. The assigned measurement uncertainty of the photosignals is the standard deviation of the mean of the readout.

Distance of the standard lamps (correction factor $\kappa_{d,S}$)

The distance of 300 mm between the lamp opening and the reference plane of the spectroradiometer has to be extended by approx. 80 mm to consider the distance from the lamp opening to the lamp center itself. The distance is set with a caliper gauge with an uncertainty of 0.05 mm (rectangular distributed). The correction factor results in $\kappa_{d,S} = 1 \pm 0.0003$.

Alignment of the standard lamps and irradiance nonuniformity (correction factor κ_ε)

The deuterium lamps are operated at a very narrow distance to the irradiated reference plane. Deuterium lamps also have a nonuniform irradiance distribution. When carefully angular and lateral aligning the lamps the correction results in $\kappa_\varepsilon = 1 \pm 0.002$ (assuming a rectangular distribution of the nonuniformity combined with the alignment).

Linearity correction $\kappa_{L,S,M}$, $\kappa_{L,M,B}$:

The photomultiplier tube shows a slight nonlinearity at higher photocurrent levels. Usually these photocurrents should be avoided and the photomultiplier should operate within the linear range. When comparing the spectral irradiance of the black-body radiator with that of deuterium lamps, a dynamic range of 10^4 has to be covered. To achieve sufficient signal-to-noise ratios, the PMT had to be operated in the nonlinear range for higher irradiances. Using the beam conjoiner method, the nonlinearity has been measured and the photocurrent could be corrected by correction factors.

Therefore the measured photocurrent v_x has to be divided by the (photocurrent-dependend) correction factor $f(v_x)$. The correction for high photocurrents is up to 1.015 and results in 1.0 for the lower range. The correction has to be applied for both, the standard lamp and the monitor lamp. Therefore the combined linearity correction factors $\kappa_{L,S,M}$ and $\kappa_{L,B,M}$ are defined as ratios of the correction factors:

$$\kappa_{L,S,M} = \frac{f(v_M)}{f(v_S)} \text{ and } \kappa_{L,M,B} = \frac{f(v_B)}{f(v_M)}.$$

For similar irradiances of the standard lamp and the (deuterium) monitor lamp $\kappa_{L,S,M} = \kappa_{L,M,B} = 1 \pm 0.001$, but when operating the blackbody, $\kappa_{L,M,B}$ can rise up to 1.015 ± 0.007 for wavelengths below 250 nm. Above 250 nm the correction factor is smaller than 1.006 ± 0.003.

Wavelength correction factor $\kappa_{\lambda,S,M}$, $\kappa_{\lambda,M,B}$

Due to the strong slope and the different gradients of the spectral irradiances of the black-body radiator and deuteriums lamps, the wavelength of the spectroradiometer has to be set very accurately to the recommended wavelengths. Both, the photocurrent of the standard lamp (or blackbody) and the monitor lamp are measured at the same wavelength setting at the same time *t* (within one minute). Therefore only the ratio of the photocurrents would have to be corrected for a potentially wrong wavelength setting. Assuming a correct wavelength setting, the wavelength correction factor for both photocurrent ratios is $\kappa_{\lambda,S,M} = \kappa_{\lambda,M,B} = 1$. The uncertainty for this assumption can be calculated from the 1st derivative of the photocurrent ratios:

$$u^2(\kappa_{\lambda,S,M}) = \left(u(\lambda) \cdot \frac{d\left(\frac{v_S(\lambda)}{v_M(\lambda)}\right) \Big/ d\lambda}{\frac{v_S(\lambda)}{v_M(\lambda)}} \right)^2 \quad \text{and} \quad u^2(\kappa_{\lambda,M,B}) = \left(u(\lambda) \cdot \frac{d\left(\frac{v_M(\lambda)}{v_B(\lambda)}\right) \Big/ d\lambda}{\frac{v_M(\lambda)}{v_B(\lambda)}} \right)^2$$

The relative change of the photocurrent ratios is shown in Figure **5.1**. For the transfer standard S as well as for the monitor lamp M deuterium lamps are used, so that their photocurrent ratio does not vary remarkably with the wavelength. Nevertheless, at 200 nm the ratios changes by 4 %/nm. This effect is due to different lamp bulb materials. When using the black-body radiator, the relative change rises up to 8 %/nm at 200 nm. The wavelength of the spectroradiometer can be set to the recommended wavelengths with an uncertainty of $u(\lambda)$ = 0,05 nm. For the deuterium lamps then, the resulting uncertainty $u(\kappa_{\lambda,S,M})$ is < 0.02 % for the wavelength region from 210 to 350 nm and is estimated to 0.2 % at 200 nm. For the black-body versus the deuterium monitor lamp, the uncertainty for the combined wavelength correction varies from 0.4 % at 200 nm to 0.2 % at 350 nm.

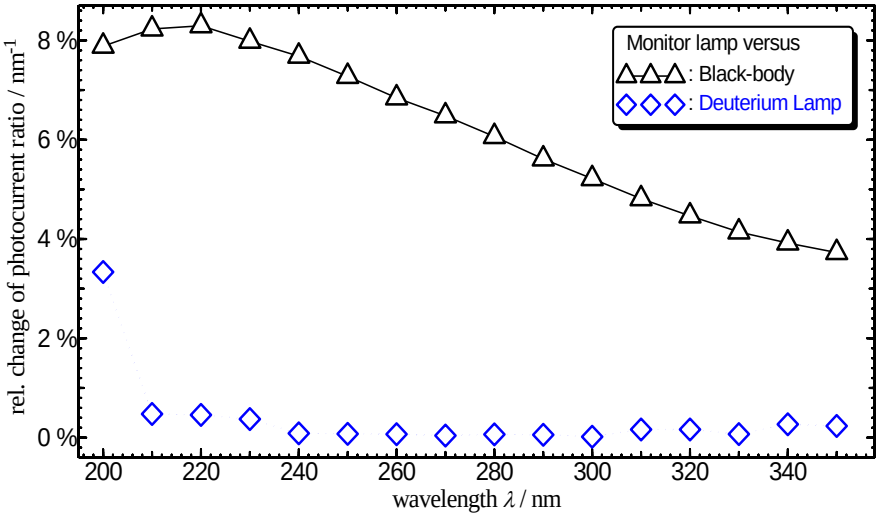

Figure 5.1 The relative spectral change of the photocurrent ratio between the monitorlamp and the black-body (triangles) or the deuterium lamps (rhombs) respectively.

Combined correction factor for spectroradiometer bandwidth ($\kappa_{b,S,M}$, $\kappa_{b,M,B}$)

Several assumptions and simplification lead to equation (5.3). The most comprehensive assumption is that the spectroradiometer is an instrument that separates only radiation of the wavelength λ_x it is set to. This simplification can be valid for very narrow-banded instruments and/or where their spectral sensitivity and the measured spectra vary only slightly or linear with wavelength. In a real monochromator system, however, the bandpass-slit function N_{mon}, the relative instrument responsivity r_{mon} and the spectral irradiance E_S of the measured standard lamp have to be considered to calculate the (true) photo-signal:

$$v_S(\lambda_x,b) = v_0(\lambda_x) \cdot \int_0^\infty N_{mon}(\lambda,\lambda_x,b) \cdot r_{mon}(\lambda,\lambda_x) \cdot E_S(\lambda)\, d\lambda \quad (5.4)$$

This equation can usually not be solved to directly get the spectral irradiance $E_S(\lambda_x)$ at the wavelength λ_x. Some ancillary conditions and measurements allow to simplify equation (5.4). The bandwidth and the slit-function of the monochromator system was measured using narrow-banded single lines of a low pressure mercury lamp. The slit-function was found to be symmetric and approximate triangular with the full width $2 \cdot b$ where b represents the bandwidth of the monochromator system. Therefore according to [8] the measured photo-signals have to be corrected by the relative change of the second derivative. This correction has to be applied to both the photo-signal assigned to the monitor-lamp and the photo-signal of the standard lamp or the working standard, respectively. It results in the correction factors

$$\kappa_{b,S,M} = \frac{1 - \frac{b^2}{12}\frac{v_S''(\lambda_x)}{v_S(\lambda_x)}}{1 - \frac{b^2}{12}\frac{v_M''(\lambda_x)}{v_M(\lambda_x)}}, \quad \kappa_{b,M,B} = \frac{1 - \frac{b^2}{12}\frac{v_M''(\lambda_x)}{v_M(\lambda_x)}}{1 - \frac{b^2}{12}\frac{v_B''(\lambda_x)}{v_B(\lambda_x)}}$$

where v_S'', v_M'' and v_B'' are the second derivatives of the photo-signals.

If the transfer standard S is of the same type as the monitor lamp M (e.g. deuterium lamp), the correction factor $\kappa_{b,S,M}$ is one. For the working standard B being a black-body radiator, $\kappa_{b,M,B}$ can vary significantly from one. In Figure 5.2 the combined correction factors for the used bandwidths of 2,9 nm (in the spectral range from 200 nm to 320 nm) and 5 nm (330 nm to 350 nm) are shown. The corrections to be applied are less than 0,7 % in the spectral range from 200 nm to 320 nm and rise up to -3 % at 350 nm.

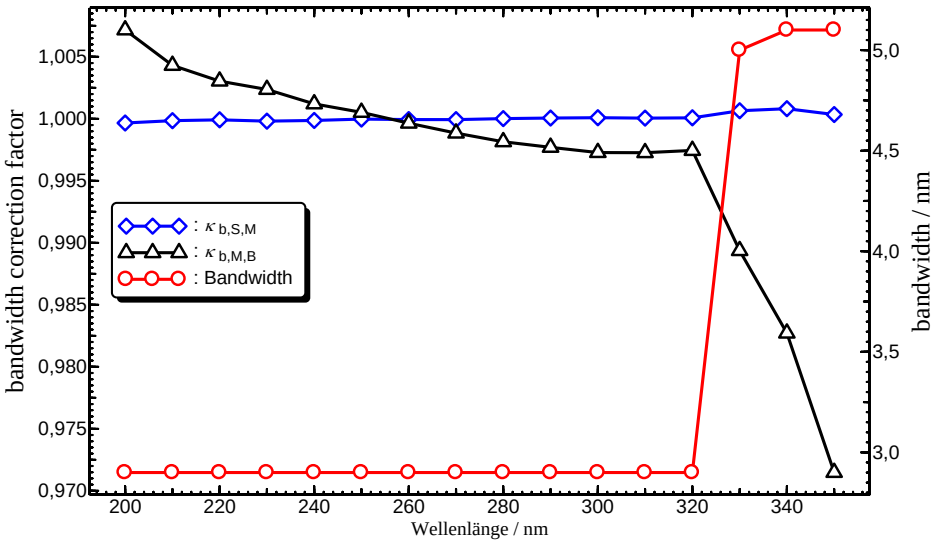

Figure 5.2 The combined bandwidth correction factors.

Correction factor for the temporal drift of the working standard or the monitor lamp κt,B,κt,M

Working standard and transfer standard were calibrated at the same place but could not be calibrated at the same time. The short term temporal drift of the standards and of the measurement

facility have to be considered. With the black-body radiator as the working standard, the spectral irradiance E_B was assigned online during the measurements and $\kappa_{t,B} = 1$. The monitor lamp was used to keep the spectral irradiance and to transfer it to the transfer standard S. Although it was photocurrent stabilized the comparison of several measurements with the black-body radiator showed a linear drift of $\delta \approx 10^{-4}$ h^{-1}. The small correction

$$\kappa_{t,M}(\lambda,t_2,t_1) = (1 + \delta(\lambda))\cdot(t_2 - t_1)$$

was applied to compare measurements that where separated more than 100 hrs in monitor lamp burning time. The uncertainty for this correction is in the range of 0,1 %.

Correction factor for electrical current settings of the lamps $\kappa_{I,S}$, $\kappa_{I,B}$, $\kappa_{I,M}$

The spectral irradiance of a lamp is strongly dependent on the electrical parameters assigned to it. Therefore it is important to set and keep the lamp current at its defined value. The DLS are equipped with a constant current power supply with a fixed lamp current of about 300 mA. The exact value might slightly vary between different power supplies and a single lamp should consequently always be operated with the same power supply. The lamp current was monitored during the measurements and turned out to change less than 0.1 mA for all lamps during all measurements. Thus, the correction factors for the electrical current are set to unity with a negligible uncertainty.

Table 5.3 Standard measurement uncertainties for spectral irradiance calibrations

Parameter		Type A Uncertainty	Type B Uncertainty	Uncertainty in Spectral Irradiance 200 nm	210 nm - 220 nm	230 nm - 240 nm	250 nm - 260 nm	270 nm - 280 nm	290 nm - 300 nm	310 nm - 320 nm	330 nm - 340 nm	350 nm
primary black-body scale realisation	E_B		0.57 K	0,38%	0,34%	0,31%	0,28%	0,26%	0,24%	0,22%	0,21%	0,20%
distance of transfer standard	$\kappa_{d,S}$		0,05 mm	0,03%	0,03%	0,03%	0,03%	0,03%	0,03%	0,03%	0,03%	0,03%
distance of working standard	$\kappa_{d,B}$		0,05 mm	0,02%	0,02%	0,02%	0,02%	0,04%	0,02%	0,02%	0,02%	0,02%
alignment of transfer standard	$\kappa_{\varepsilon,S}$		0,2%	0,2%	0,2%	0,2%	0,2%	0,2%	0,2%	0,2%	0,2%	0,2%
alignment of working standard	$\kappa_{\varepsilon,B}$		0,03%	0,03%	0,03%	0,03%	0,03%	0,03%	0,03%	0,03%	0,03%	0,03%
bandwidth correction factor	$\kappa_{b,S,M}$		0,05% - 0,1%	0,1%	0,05%	0,05%	0,05%	0,05%	0,05%	0,05%	0,05%	0,3%
bandwidth correction factor	$\kappa_{b,M,B}$		0,05% - 0,1%	0,1%	0,05%	0,05%	0,05%	0,05%	0,05%	0,05%	0,05%	0,3%
wavelength for transfer standard	$\kappa_{\lambda,S,M}$		0.05 nm	0,17%	0,02%	0,02%	0,01%	0,01%	0,01%	0,01%	0,01%	0,01%
wavelength for working standard	$\kappa_{\lambda,B,M}$		0.05 nm	0,39%	0,41%	0,40%	0,36%	0,32%	0,28%	0,24%	0,21%	0,19%
stability of facility and monitor lamp	$\kappa_{t,M}$	0,1%		0,10%	0,10%	0,10%	0,10%	0,10%	0,10%	0,10%	0,10%	0,10%
standard deviation of working standard	v_B	0,2 – 1,4%		1,4%	0,8%	0,4%	0,2%	0,2%	0,2%	0,2%	0,2%	0,3%
standard deviation of transfer standard	v_S	0,1% - 1%		0,1%	0,1%	0,1%	0,1%	0,2%	0,3%	0,4%	0,5%	1%
reproducibility of transfer standard	E_S	0,2% - 0,7%		0,5%	0,4%	0,30%	0,20%	0,2%	0,3%	0,3%	0,5%	0,7%
total standard measurement uncertainty				1,6%	1,1%	0,8%	0,6%	0,6%	0,6%	0,7%	0,8%	1,3%
Expanded uncertainty (k=2)				3,2%	2,2%	1,5%	1,2%	1,2%	1,2%	1,4%	1,6%	2,6%

6. Results of Measurements

As it was described in section 2.2 originally two VNIIOFI measurement rounds and one PTB round were planned in the following sequence: VNIIOFI – PTB – VNIIOFI. However, because of poor ag reement between the first and second VNIIOFI rounds and a distance error at the PTB first round, more measurements were performed and the actual sequence was the following:

VNIIOFI #1 – PTB #1 – VNIIOFI #2 – VNIIOFI #3 – VNIIOFI #4 – PTB #2 – VNIIOFI #5

Below the results of all measurement rounds are presented. **However, only the VNIIOFI rounds #3, #4 and #5, and PTB round #2 were selected after Pre-Draft A for evaluating the comparison results.**

6.1. Lamp system electrical stability

The average lamp voltages and lamp current measured at each round of measurements are presented in Table 6.1 (for VNIIOFI measurements) and Table 6.2 (for PTB measurements).

Table 6.1. Average Lamp voltages and currents measured at VNIIOFI

Round#	Lamp system DL1		Lamp system DL2		Lamp system DL3	
	Current, mA	Voltage, V	Current, mA	Voltage, V	Current, mA	Voltage, V
VNIIOFI round #1	319.63	76.6	318.93	82.8	318.92	77.5
VNIIOFI round #2	319.76	77.0	318.87	82.5	318.93	76.7
VNIIOFI round #3	319.64	76.8	318.93	83.2	318.95	76.7
VNIIOFI round #4	319.67	76.9	318.95	84.1	319.04	76.7
VNIIOFI round #5	319.77	76.2	-	-	319.11	76.6

Table 6.2. Average Lamp voltages and currents measured at PTB

Round#	Lamp system DL1		Lamp system DL2		Lamp system DL3	
	Current, mA	Voltage, V	Current, mA	Voltage, V	Current, mA	Voltage, V
PTB round #1	319.7	76.6	318.8	83.1	318.9	76.6
PTB round #2	319.6	77.2	318.8	82.4	318.9	76.6

6.2. Results of VNIIOFI measurement

Within each round VNIOOFI performed three to four independent measurement of each lamp. Here, only averaged values for a lamp and round are reported. Standard deviations of the independent measurements are included in the Type A uncertainty (see section 4.4). Tables 6.3, 6.4 and 6.5 presented the reported VNIIOFI data of measured spectral irradiance for the lamps DL1, DL2 and DL3, respectively. The measurements for the lamp DL2 in round #5 could not be performed due to a failure of the lamp system.

Although the comparison COOMET.PR-K1b.1, following CCPR-K1b, was carried out in the wavelength range from 200 nm to 350 nm, VNIIOFI performed measurements in the spectral range from 200 nm to 400 nm. We present here all measured wavelength results including 360 nm to 400 nm although it was not the subject of the comparison.

Table 6.3. VNIIOFI measured results for Lamp system DL1 at distance of 400 mm

λ Wavelength, nm	$E_\lambda(\lambda)$ Spectral Irradiance, W $m^{-2}nm^{-1}$				
	Round #1	Round #2	Round #3	Round #4	Round #5
200	6.477E-04	5.221E-04	7.561E-04	7.246E-04	6.985E-04
210	7.208E-04	6.645E-04	7.538E-04	7.512E-04	7.521E-04
220	7.086E-04	6.526E-04	7.102E-04	7.154E-04	7.091E-04
230	6.401E-04	5.809E-04	6.443E-04	6.356E-04	6.282E-04
240	5.632E-04	5.206E-04	5.640E-04	5.571E-04	5.525E-04
250	4.907E-04	4.507E-04	4.894E-04	4.851E-04	4.817E-04
260	4.199E-04	3.864E-04	4.207E-04	4.174E-04	4.162E-04
270	3.570E-04	3.310E-04	3.579E-04	3.545E-04	3.529E-04
280	3.020E-04	2.814E-04	3.029E-04	2.996E-04	2.976E-04
290	2.543E-04	2.379E-04	2.550E-04	2.520E-04	2.499E-04
300	2.151E-04	2.008E-04	2.156E-04	2.156E-04	2.140E-04
310	1.838E-04	1.723E-04	1.840E-04	1.827E-04	1.830E-04
320	1.596E-04	1.496E-04	1.593E-04	1.580E-04	1.582E-04
330	1.393E-04	1.312E-04	1.396E-04	1.384E-04	1.389E-04
340	1.229E-04	1.164E-04	1.233E-04	1.221E-04	1.223E-04
350	1.096E-04	1.035E-04	1.094E-04	1.090E-04	1.0823E-04
360	9.785E-05	9.269E-05	9.816E-05	9.763E-05	9.680E-05
370	8.895E-05	8.426E-05	8.936E-05	8.863E-05	8.814E-05
380	8.236E-05	7.835E-05	8.257E-05	8.194E-05	8.169E-05
390	7.352E-05	6.997E-05	7.353E-05	7.361E-05	7.363E-05
400	6.857E-05	6.482E-05	6.866E-05	6.897E-05	6.862E-05

Table 6.4. VNIIOFI measured results for Lamp system DL2 at distance of 400 mm

λ Wavelength, nm	$E_\lambda(\lambda)$ Spectral Irradiance, W $m^{-2}nm^{-1}$				
	Round #1	Round #2	Round #3	Round #4	Round #5
200	5.563E-04	4.372E-04	6.073E-04	6.092E-04	-
210	6.099E-04	5.790E-04	6.237E-04	6.137E-04	-
220	5.857E-04	5.564E-04	5.784E-04	5.793E-04	-
230	5.356E-04	5.036E-04	5.215E-04	5.212E-04	-
240	4.711E-04	4.347E-04	4.583E-04	4.588E-04	-
250	4.088E-04	3.795E-04	3.979E-04	3.986E-04	-
260	3.496E-04	3.271E-04	3.429E-04	3.426E-04	-
270	2.976E-04	2.796E-04	2.920E-04	2.924E-04	-
280	2.532E-04	2.379E-04	2.493E-04	2.490E-04	-
290	2.140E-04	2.025E-04	2.110E-04	2.108E-04	-
300	1.825E-04	1.730E-04	1.797E-04	1.797E-04	-
310	1.570E-04	1.494E-04	1.551E-04	1.547E-04	-
320	1.370E-04	1.306E-04	1.352E-04	1.348E-04	-
330	1.205E-04	1.152E-04	1.191E-04	1.189E-04	-
340	1.071E-04	1.028E-04	1.059E-04	1.056E-04	-
350	9.549E-05	9.136E-05	9.461E-05	9.443E-05	-
360	8.573E-05	8.264E-05	8.495E-05	8.442E-05	-
370	7.812E-05	7.504E-05	7.739E-05	7.704E-05	-
380	7.223E-05	6.927E-05	7.146E-05	7.116E-05	-
390	6.471E-05	6.264E-05	6.412E-05	6.389E-05	-
400	5.998E-05	5.759E-05	5.909E-05	5.927E-05	-

Table 6.5. VNIIOFI measured results for Lamp system DL3 at distance of 400 mm

λ Wavelength, nm	$E_\lambda(\lambda)$ Spectral Irradiance, W $m^{-2}nm^{-1}$				
	Round #1	Round #2	Round #3	Round #4	Round #5
200	5.689E-04	4.739E-04	6.550E-04	6.502E-04	6.195E-04
210	6.483E-04	6.197E-04	6.685E-04	6.702E-04	6.615E-04
220	6.407E-04	5.955E-04	6.300E-04	6.285E-04	6.258E-04
230	5.928E-04	5.536E-04	5.749E-04	5.765E-04	5.758E-04
240	5.253E-04	4.874E-04	5.084E-04	5.108E-04	5.074E-04
250	4.591E-04	4.267E-04	4.434E-04	4.448E-04	4.405E-04
260	3.943E-04	3.704E-04	3.838E-04	3.832E-04	3.788E-04
270	3.374E-04	3.177E-04	3.276E-04	3.280E-04	3.261E-04
280	2.871E-04	2.698E-04	2.796E-04	2.786E-04	2.758E-04
290	2.428E-04	2.283E-04	2.361E-04	2.364E-04	2.353E-04
300	2.050E-04	1.938E-04	2.007E-04	2.007E-04	1.996E-04
310	1.759E-04	1.667E-04	1.721E-04	1.720E-04	1.701E-04
320	1.524E-04	1.447E-04	1.496E-04	1.494E-04	1.480E-04
330	1.334E-04	1.273E-04	1.313E-04	1.310E-04	1.305E-04
340	1.179E-04	1.131E-04	1.160E-04	1.160E-04	1.147E-04
350	1.047E-04	1.008E-04	1.037E-04	1.036E-04	1.025E-04
360	9.347E-05	9.042E-05	9.296E-05	9.291E-05	9.176E-05
370	8.486E-05	8.219E-05	8.477E-05	8.449E-05	8.419E-05
380	7.812E-05	7.638E-05	7.855E-05	7.833E-05	7.800E-05
390	6.975E-05	6.875E-05	7.048E-05	7.048E-05	6.995E-05
400	6.482E-05	6.338E-05	6.546E-05	6.547E-05	6.500E-05

Figures 6.1, 6.2 and 6.3 shows repeatability of VNIIOFI measurement in a form of relative deviations of VNIIOFI measured spectral irradiance values in each round from the values measured in the round #4. The deviations were calculated separately for each lamp as $\left(E_{\lambda\,j,\mathrm{round}}(\lambda)/E_{\lambda\,j,4}(\lambda)-1\right)\cdot 100\%$, where $E_{\lambda\,j,\mathrm{round}}(\lambda)$ is the average spectral irradiance measured at the VNIIOFI round # for the lamps *j*, and $E_{\lambda\,j,4}(\lambda)$ is the average spectral irradiance measured at the VNIIOFI round #4 for the same lamps. The blue dash lines in the figures indicate VNIIOFI expanded measurement uncertainties in the round #4 for k = 2 and k = 3.

One can see that the VNIIOFI results for the round #2 are inconsistent with the other rounds. Therefore the participants agreed excluding the VNIIOFI round # 2 results from the further comparison analysis.

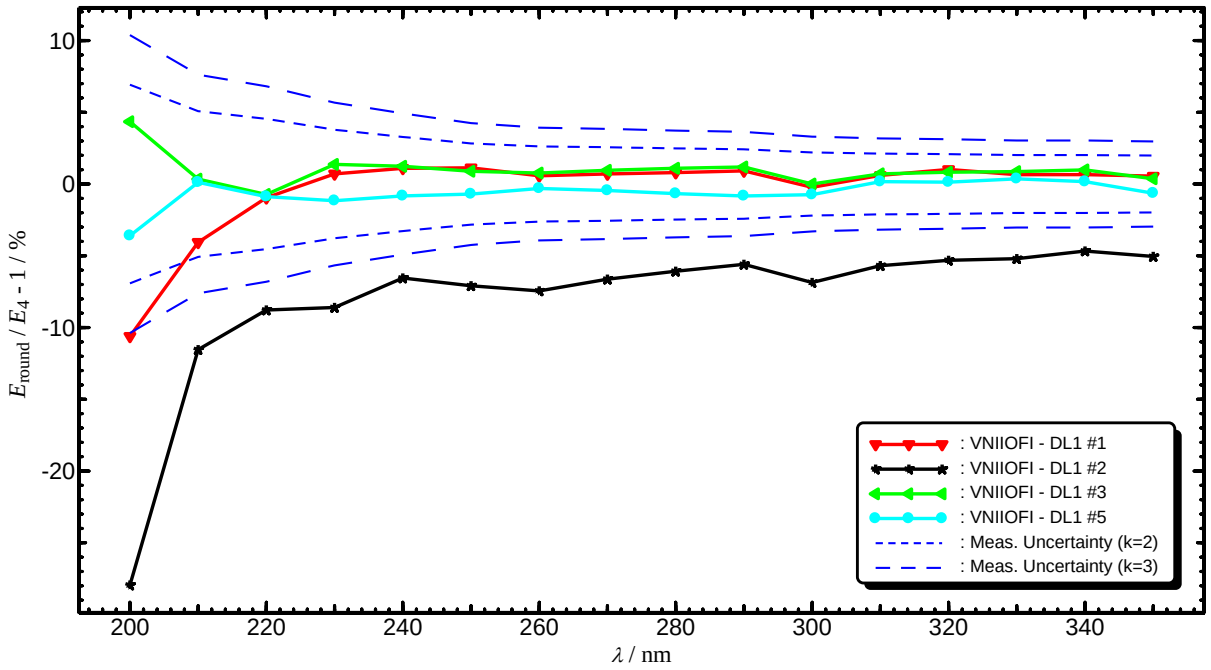

Figure 6.1 Deviation of the lamp DL1 spectral irradiance values measured at VNIIOFI in each round from the values measured in the round # 4. The blue dash lines indicate the expanded measurement uncertainties in round #4 for k = 2 and k = 3.

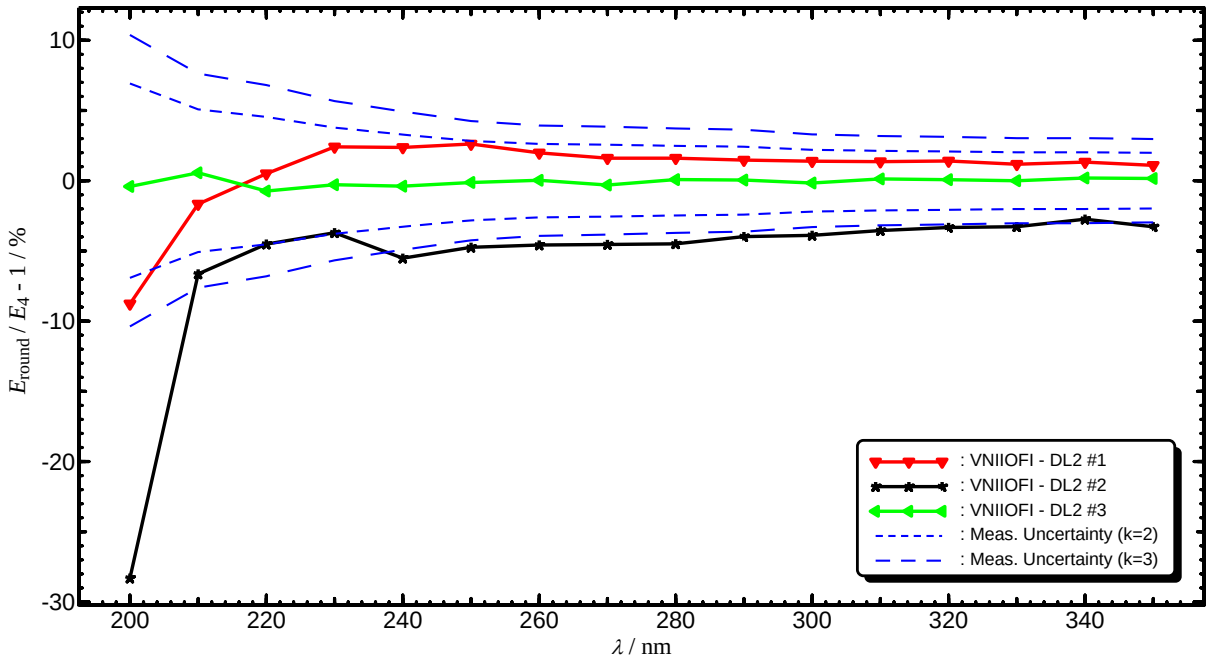

Figure 6.2 Deviation of the lamp DL2 spectral irradiance values measured at VNIIOFI in each round from the values measured in the round # 4. The blue dash lines indicate the expanded measurement uncertainties in round #4 for k = 2 and k = 3.

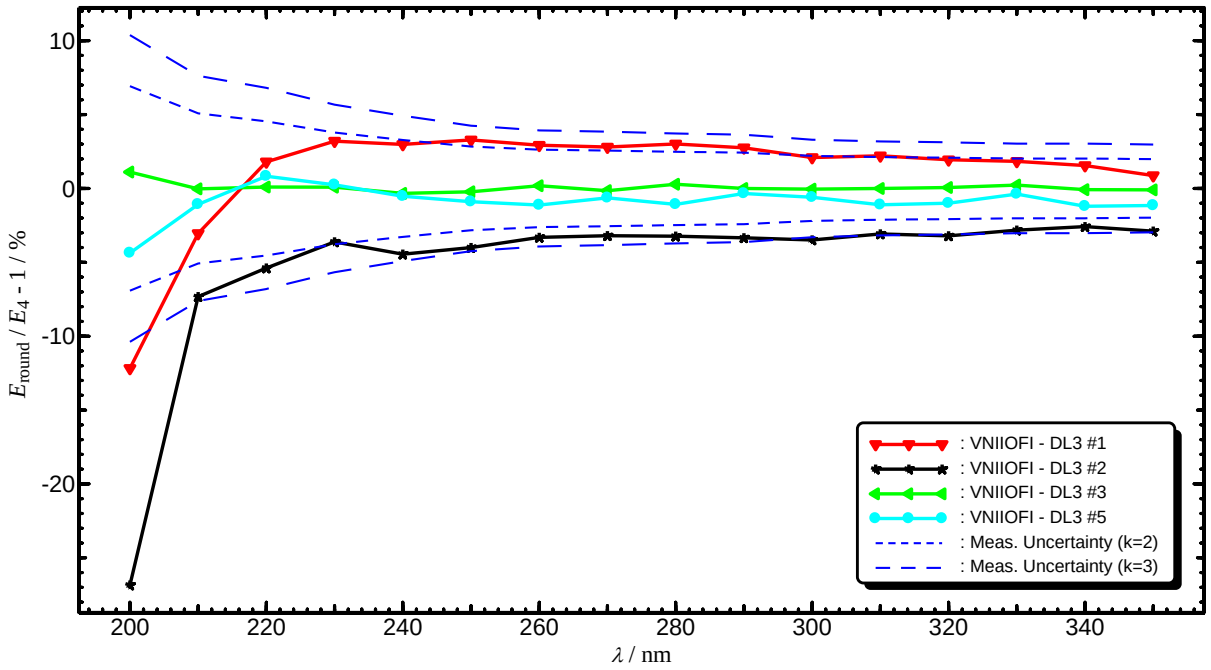

Figure 6.3 Deviation of the lamp DL3 spectral irradiance values measured at VNIIOFI in each round from the values measured in the round # 4. The blue dash lines indicate the expanded measurement uncertainties in round #4 for k = 2 and k = 3.

6.3. Results of PTB (link)

The measurements at the PTB Round #1 were carried out the distance of 300 mm instead of 400 mm as requested by the Technical Protocol. Therefore, the spectral irradiance data of the PTB Round #1 had to be corrected. The correction factor is different for every lamp and was obtained during the PTB Round #2 when PTB measured spectral irradiance of all lamps at both distances, 300 mm and 400 mm. The (corrected) PTB values of spectral irradiance at the distance of 400 mm are presented in Tables 6.6.

PTB results of spectral irradiance measured at the distance of 300 mm in both PTB rounds are presented in Table 6.7 and can also be used for analysis of the lamp stability.

Repeatability of PTB measurements is shown in Figure 6.4 in a form of relative differences between the spectral irradiance values measured in the PTB round #1 and the PTB round #2, and calculated as $\left(E_{\lambda,j,\mathrm{round}}(\lambda)/E_{\lambda,j,2}(\lambda)-1\right)\cdot 100\%$, where $E_{\lambda,j,\mathrm{round}}(\lambda)$ is the average spectral irradiance measured at the PTB round #1 for the lamps *j*, and $E_{\lambda,j,2}(\lambda)$ is the average spectral irradiance measured at the PTB round #2 for the same lamps. One can see that the PTB measurement results for the lamp DL1 of the round # 1 is not consistent with other results.

Table 6.6. PTB measured results at distance of 400 mm

λ Wavelength, nm	Spectral Irradiance $E_\lambda(\lambda)$, W $m^{-2}nm^{-1}$					
	Lamp DL1		Lamp DL2		Lamp DL3	
	PTB Round #1	PTB Round #2	PTB Round #1	PTB Round #2	PTB Round #1	PTB Round #2
200	7.884E-04	7.464E-04	6.107E-04	6.129E-04	6.655E-04	6.621E-04
210	7.923E-04	7.526E-04	6.166E-04	6.185E-04	6.737E-04	6.714E-04
220	7.390E-04	7.095E-04	5.771E-04	5.779E-04	6.403E-04	6.386E-04
230	6.594E-04	6.435E-04	5.221E-04	5.236E-04	5.880E-04	5.846E-04
240	5.786E-04	5.642E-04	4.580E-04	4.580E-04	5.182E-04	5.160E-04
250	4.981E-04	4.845E-04	3.946E-04	3.949E-04	4.466E-04	4.456E-04
260	4.223E-04	4.117E-04	3.367E-04	3.369E-04	3.824E-04	3.812E-04
270	3.582E-04	3.495E-04	2.876E-04	2.870E-04	3.255E-04	3.243E-04
280	3.040E-04	2.966E-04	2.444E-04	2.447E-04	2.775E-04	2.765E-04
290	2.572E-04	2.515E-04	2.093E-04	2.094E-04	2.366E-04	2.359E-04
300	2.181E-04	2.142E-04	1.802E-04	1.800E-04	2.028E-04	2.022E-04
310	1.888E-04	1.850E-04	1.567E-04	1.567E-04	1.752E-04	1.747E-04
320	1.632E-04	1.600E-04	1.371E-04	1.367E-04	1.522E-04	1.518E-04
330	1.428E-04	1.402E-04	1.207E-04	1.203E-04	1.338E-04	1.334E-04
340	1.255E-04	1.236E-04	1.070E-04	1.068E-04	1.180E-04	1.176E-04
350	1.112E-04	1.094E-04	9.491E-05	9.474E-05	1.051E-04	1.046E-04

Table 6.7. PTB measured results at distance of 300 mm

λ Wavelength, nm	Spectral Irradiance $E_\lambda(\lambda)$, W $m^{-2}nm^{-1}$					
	Lamp DL1		Lamp DL2		Lamp DL3	
	PTB Round #1	PTB Round #2	PTB Round #1	PTB Round #2	PTB Round #1	PTB Round #2
200	1.332E-03	1.261E-03	1.110E-03	1.114E-03	1.208E-03	1.202E-03
210	1.336E-03	1.269E-03	1.115E-03	1.118E-03	1.225E-03	1.221E-03
220	1.249E-03	1.199E-03	1.035E-03	1.036E-03	1.152E-03	1.149E-03
230	1.113E-03	1.086E-03	9.194E-04	9.220E-04	1.035E-03	1.029E-03
240	9.762E-04	9.518E-04	8.043E-04	8.043E-04	9.128E-04	9.089E-04
250	8.400E-04	8.171E-04	6.929E-04	6.934E-04	7.884E-04	7.865E-04
260	7.136E-04	6.957E-04	5.882E-04	5.885E-04	6.703E-04	6.682E-04
270	6.054E-04	5.908E-04	4.992E-04	4.981E-04	5.700E-04	5.678E-04
280	5.113E-04	4.989E-04	4.245E-04	4.251E-04	4.830E-04	4.813E-04
290	4.337E-04	4.241E-04	3.618E-04	3.620E-04	4.101E-04	4.089E-04
300	3.692E-04	3.626E-04	3.102E-04	3.099E-04	3.501E-04	3.491E-04
310	3.179E-04	3.115E-04	2.691E-04	2.690E-04	3.016E-04	3.008E-04
320	2.751E-04	2.696E-04	2.344E-04	2.338E-04	2.610E-04	2.602E-04
330	2.405E-04	2.362E-04	2.064E-04	2.058E-04	2.287E-04	2.279E-04
340	2.115E-04	2.082E-04	1.825E-04	1.822E-04	2.014E-04	2.007E-04
350	1.873E-04	1.843E-04	1.624E-04	1.621E-04	1.787E-04	1.779E-04

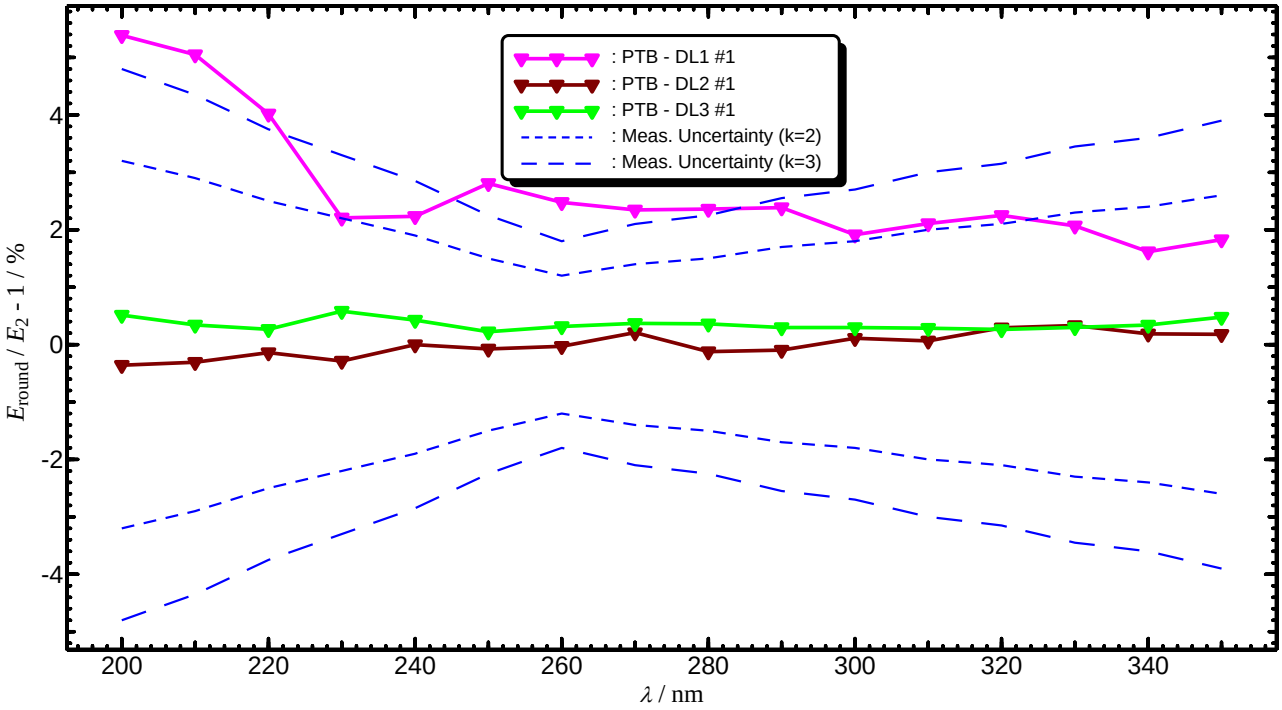

Figure 6.4 Repeatability of PTB measurement: persentage differences of round # 1 to round # 2. The blue dash lines indicate the PTB expanded measurement uncertainties for k = 2 and k = 3.

7. Pre-Draft A

According to the CCPR-G5 [2] PTB as a link laboratory was responsible for caring out Pre-Draft A procedures that included three stages: 1) verification of VNIIOFI reported data, 2) analysis of VNIIOFI uncertainty budget and 3) calculation and analysis of Relative Data.

7.1 Relative Data

First the repeatability of VNIIOFI data, presented in Figures 6.1 – 6.3, was discussed. The participants agreed to exclude the VNIIOFI round #2 data from the further analysis including the relative data.

The relative data were calculated by PTB in the following way:

The results reported by VNIIOFI for all rounds *k* were averaged for every lamp:

$$E_{\lambda,\mathrm{VNIIOFI},j}(\lambda)=\frac{1}{R}\sum_{k=1}^{R}E_{\lambda,\mathrm{VNIIOFI}\,k,j}(\lambda) \qquad (7.1)$$

where $E_{\lambda,\mathrm{VNIIOFI},j}(\lambda)$ is the VNIIOFI overall averaged spectral irradiance of the lamp *j* and $E_{\lambda,\mathrm{VNIIOFI}\,k,j}(\lambda)$ are the spectral irradiance values for each round *k* as reported by VNIIOFI.

These results were then compared to the spectral irradiances assigned by the PTB during round *m* of the pilot's measurements. This operation eliminates a possible linear drift of the lamps between the measurement rounds. At this stage of Pre-Draft A, no absolute deviations have been presented. Therefore, the relative data was calculated as normalized difference for each lamp:

$$\delta_j(\lambda) = \left(\frac{\frac{E_{\lambda,\mathrm{VNIIOFI},j}(\lambda)}{E_{\lambda,\mathrm{PTB}\,m,j}(\lambda)}}{\frac{1}{N}\sum_{j=1}^{N}\frac{E_{\lambda,\mathrm{VNIIOFI},j}(\lambda)}{E_{\lambda,\mathrm{PTB}\,m,j}(\lambda)}} - 1 \right) \cdot 100\% \qquad (7.2)$$

Here N=3 is the number of lamps. The relative data $\delta_j(\lambda)$ can give an indication of outliers or unexpected results.

The relative data were calculated separately for two stages of the comparison:

1) The first stage includes the following measurement rounds: VNIIOFI round #1, PTB round #1 and VNIIOFI round #3; in this case relative data compares the average results of the VNIIOFI rounds #1 and #3 to the results of the PTB round #1. The first stage relative data are presented in Figure 7.1.

2) The second stage includes the measurement rounds: VNIIOFI round #3, VNIIOFI round #4, PTB round #2 and VNIIOFI round #5; in this case relative data compares the average results of the VNIIOFI rounds #3, #4 and #5 and the results of the PTB round #2. The second stage relative data are presented in Figure 7.2.

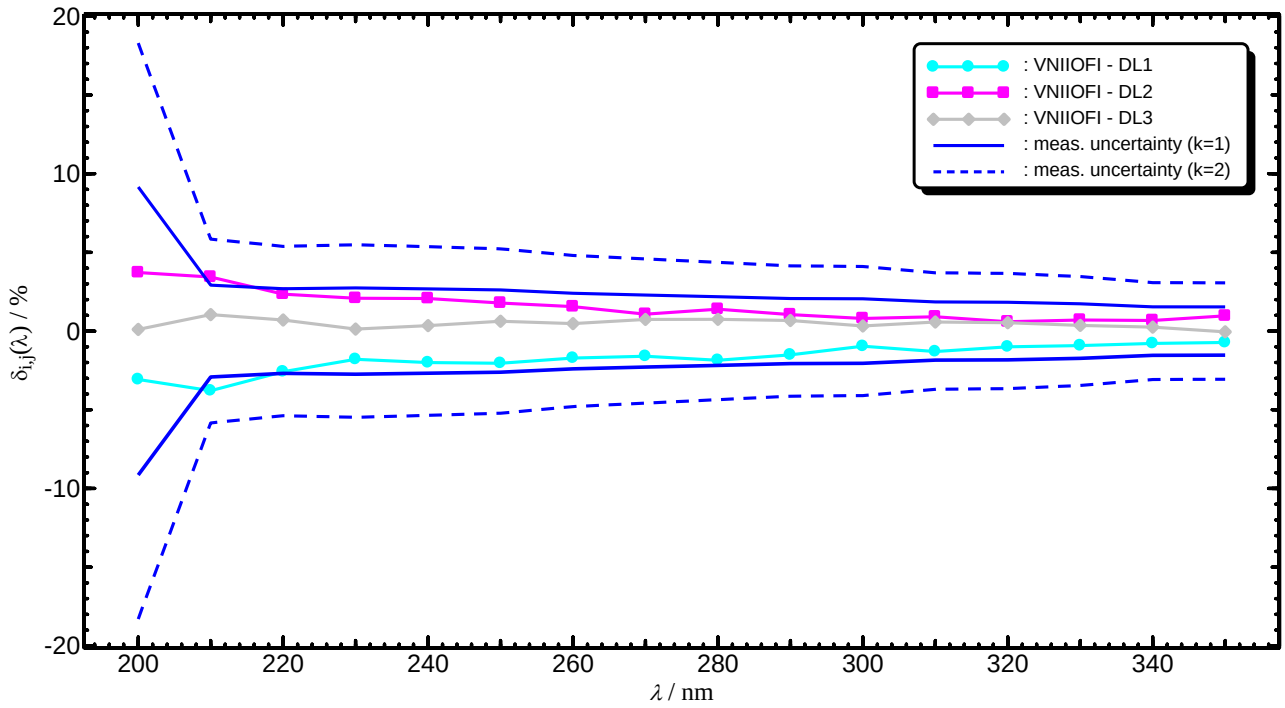

Figure 7.1. Relative data calculated for the following measurement rounds: VNIIOFI rounds #1 and #3, and PTB round #1. The blue lines indicate the VNIIOFI round #1 measurement uncertainties for k = 1 and k = 2.

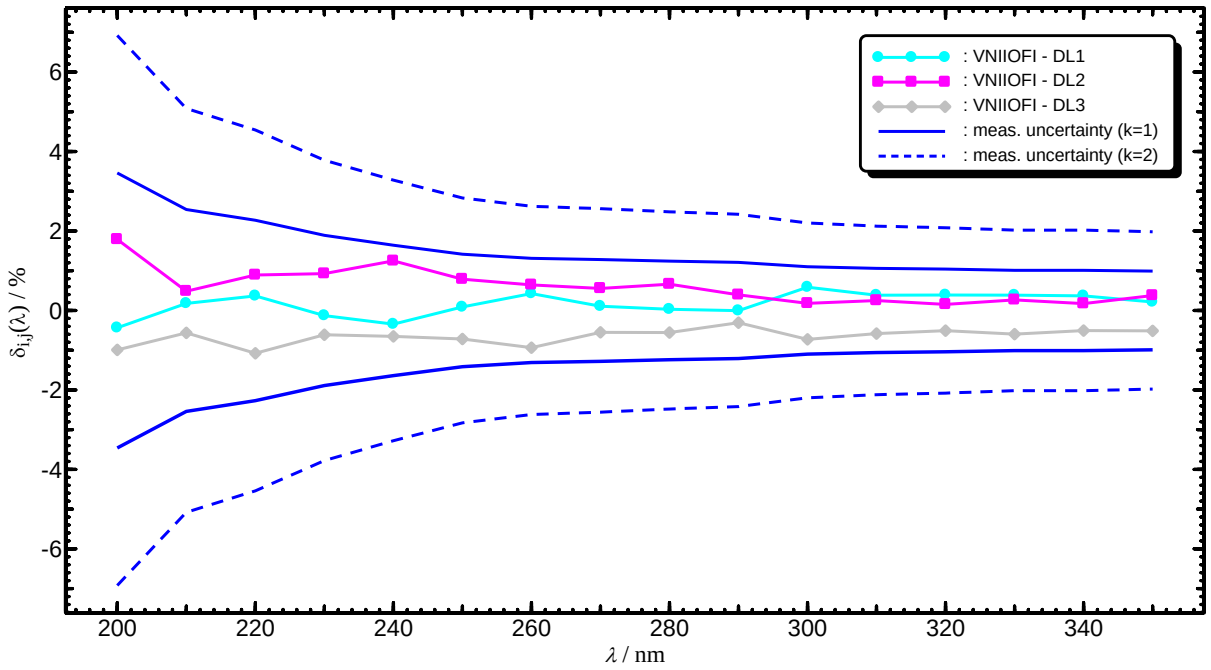

Figure 7.2. Relative data calculated for the following measurement rounds: VNIIOFI rounds #3, #4 and #5, and PTB round #2. The blue lines indicate the VNIIOFI rounds #3 to #5 measurement uncertainties for $k = 1$ and $k = 2$.

Based on the relative data and taking into account the poor repeatability of the VNIIOFI rounds #1 and #2 for all lamps and the PTB round #1 for the lamp DL1, as well as the error in distance of the PTB round #1, the participants agreed excluding from the further comparison analysis the measurement data of the VNIIOFI rounds #1 and #2 and of the PTB round #1.

8. Results of Measurements after Pre-Draft A

At the Pre-Draft A stage some measurement results were excluded. Tables 8.1, 8.2 and 8.3 summarises the results of measurements used for evaluated of the comparison results.

Table 8.1. Lamp system DL1. Results of Spectral Irradiance at distance of 400 mm

λ Wavelength, nm	$E_\lambda(\lambda)$ Spectral Irradiance, W $m^{-2}nm^{-1}$			
	VNIIOFI Round #3	VNIIOFI Round #4	VNIIOFI Round #5	PTB Round #2
200	7.561E-04	7.246E-04	6.985E-04	7.481E-04
210	7.538E-04	7.512E-04	7.521E-04	7.541E-04
220	7.102E-04	7.154E-04	7.091E-04	7.116E-04
230	6.443E-04	6.356E-04	6.282E-04	6.448E-04
240	5.640E-04	5.571E-04	5.525E-04	5.645E-04
250	4.894E-04	4.851E-04	4.817E-04	4.849E-04
260	4.207E-04	4.174E-04	4.162E-04	4.120E-04
270	3.579E-04	3.545E-04	3.529E-04	3.495E-04
280	3.029E-04	2.996E-04	2.976E-04	2.971E-04
290	2.550E-04	2.520E-04	2.499E-04	2.523E-04
300	2.156E-04	2.156E-04	2.140E-04	2.140E-04
310	1.840E-04	1.827E-04	1.830E-04	1.853E-04
320	1.593E-04	1.580E-04	1.582E-04	1.601E-04
330	1.396E-04	1.384E-04	1.389E-04	1.401E-04
340	1.233E-04	1.221E-04	1.223E-04	1.235E-04
350	1.094E-04	1.090E-04	1.082E-04	1.096E-04

Table 8.2. Lamp system DL2. Results of Spectral Irradiance at distance of 400 mm

λ Wavelength, nm	$E_\lambda(\lambda)$ Spectral Irradiance, W $m^{-2}nm^{-1}$			
	VNIIOFI Round #3	VNIIOFI Round #4	VNIIOFI Round #5	PTB Round #2
200	6.073E-04	6.092E-04	-	6.133E-04
210	6.237E-04	6.137E-04	-	6.175E-04
220	5.784E-04	5.793E-04	-	5.798E-04
230	5.215E-04	5.212E-04	-	5.237E-04
240	4.583E-04	4.588E-04	-	4.575E-04
250	3.979E-04	3.986E-04	-	3.949E-04
260	3.429E-04	3.426E-04	-	3.367E-04
270	2.920E-04	2.924E-04	-	2.865E-04
280	2.493E-04	2.490E-04	-	2.444E-04
290	2.110E-04	2.108E-04	-	2.091E-04
300	1.797E-04	1.797E-04	-	1.802E-04
310	1.551E-04	1.547E-04	-	1.562E-04
320	1.352E-04	1.348E-04	-	1.364E-04
330	1.191E-04	1.189E-04	-	1.202E-04
340	1.059E-04	1.056E-04	-	1.067E-04
350	9.461E-05	9.443E-05	-	9.451E-05

Table 8.3. Lamp system DL3. Results of Spectral Irradiance at distance of 400 mm

λ Wavelength, nm	$E_\lambda(\lambda)$ Spectral Irradiance, W $m^{-2}nm^{-1}$			
	VNIIOFI Round #3	VNIIOFI Round #4	VNIIOFI Round #5	PTB Round #2
200	6.550E-04	6.502E-04	6.195E-04	6.618E-04
210	6.685E-04	6.702E-04	6.615E-04	6.716E-04
220	6.300E-04	6.285E-04	6.258E-04	6.393E-04
230	5.749E-04	5.765E-04	5.758E-04	5.843E-04
240	5.084E-04	5.108E-04	5.074E-04	5.162E-04
250	4.434E-04	4.448E-04	4.405E-04	4.456E-04
260	3.838E-04	3.832E-04	3.788E-04	3.805E-04
270	3.276E-04	3.280E-04	3.261E-04	3.241E-04
280	2.796E-04	2.786E-04	2.758E-04	2.763E-04
290	2.361E-04	2.364E-04	2.353E-04	2.358E-04
300	2.007E-04	2.007E-04	1.996E-04	2.020E-04
310	1.721E-04	1.720E-04	1.701E-04	1.749E-04
320	1.496E-04	1.494E-04	1.480E-04	1.517E-04
330	1.313E-04	1.310E-04	1.305E-04	1.336E-04
340	1.160E-04	1.160E-04	1.147E-04	1.177E-04
350	1.037E-04	1.036E-04	1.025E-04	1.046E-04

9. Comparison results

9.1 VNIIOFI to PTB difference

Relative differences $\Delta_{\mathrm{VNIIOFI-PTB},j}(\lambda)$ between the VNIIOFI and PTB measurement results for lamp *j* were calculated as

$$\Delta_{\mathrm{VNIIOFI-PTB},j}(\lambda)=\left(\frac{E_{\lambda,\mathrm{VNIIOFI},j}(\lambda)}{E_{\lambda,PTB,j}(\lambda)}-1\right)\cdot 100\% \tag{9.1}$$

where

$$E_{\lambda,\mathrm{VNIIOFI},j}(\lambda)=\frac{1}{3}\left(E_{\lambda,\mathrm{VNIIOFI\,\#3},j}(\lambda)+E_{\lambda,\mathrm{VNIIOFI\,\#4},j}(\lambda)+E_{\lambda,\mathrm{VNIIOFI\,\#5},j}(\lambda)\right), \tag{9.2}$$

$$E_{\lambda,\mathrm{PTB},j}(\lambda)=E_{\lambda,\mathrm{PTB\,\#2},j}(\lambda), \tag{9.3}$$

and $E_{\lambda,\mathrm{VNIIOFI\,\#3},j}(\lambda)$, $E_{\lambda,\mathrm{VNIIOFI\,\#4},j}(\lambda)$, $E_{\lambda,\mathrm{VNIIOFI\,\#4},j}(\lambda)$ and $E_{\lambda,\mathrm{PTB\,\#2},j}(\lambda)$ are the average spectral irradiance values presented in the Tables 8.1, 8.2 and 8.3 for the measurement rounds VNIIOFI #3, VNIIOFI #4, VNIIOGI #5 and PTB #2, respectively.

Final values of VNIIOFI to PTB differences $\Delta_{\mathrm{VNIIOFI-PTB}}(\lambda)$ were calculated as averages of $\Delta_{\mathrm{VNIIOFI-PTB},j}(\lambda)$ for all three lamps:

$$\Delta_{\mathrm{VNIIOFI-PTB}}(\lambda)=\frac{1}{3}\sum_{j=1}^{3}\Delta_{\mathrm{VNIIOFI-PTB},j}(\lambda) \tag{9.4}$$

Standard uncertainties of the VNIIOFI to PTB differences $u_{\mathrm{VNIIOFI-PTB}}(\lambda)$ were calculated as a square-root of the square sum of the VNIIOFI and PTB measurement uncertainties:

$$u_{\mathrm{VNIIOFI-PTB}}(\lambda)=\sqrt{u^2_{VNIIOFI}(\lambda)+u^2_{PTB}(\lambda)}, \tag{9.5}$$

where $u_{\mathrm{VNIIOFI}}(\lambda)$ and $u_{\mathrm{PTB}}(\lambda)$ are presented in Table 4.6 and Table 5.3, respectively. Expanded uncertainty of the VNIIOFI to PTB differences were calculated as

$$U_{\mathrm{VNIIOFI-PTB}}(\lambda)=2\cdot u_{\mathrm{VNIIOFI-PTB}}(\lambda) \tag{9.6}$$

The values of VNIIOFI to PTB differences are presented in Table 9.1 and Figure 9.1.

Table 9.1. VNIIOFI to PTB Differences

λ Wavelength nm	$\Delta_{VNIIOFI-PTB,j}(\lambda)$, %			$\Delta_{VNIIOFI-PTB}(\lambda)$ %	$u_{VNIIOFI-PTB}(\lambda)$ %	$U_{VNIIOFI-PTB}(\lambda)$ %
	Lamp DL1	Lamp DL2	Lamp DL3			
200	-2.7	-0.8	-3.1	-2.2	3.8	7.6
210	0.0	0.0	-0.7	-0.2	2.8	5.5
220	0.3	0.2	-1.6	-0.4	2.5	5.1
230	-1.2	-0.4	-1.5	-1.0	2.1	4.1
240	-1.1	0.1	-1.4	-0.8	1.8	3.6
250	0.2	0.9	-0.6	0.2	1.6	3.1
260	1.6	1.8	0.2	1.2	1.4	2.9
270	1.6	1.8	0.9	1.4	1.4	2.8
280	1.2	1.8	0.5	1.2	1.4	2.8
290	0.3	0.7	0.0	0.4	1.4	2.7
300	0.4	-0.2	-0.9	-0.2	1.3	2.5
310	-0.9	-1.1	-1.9	-1.3	1.3	2.5
320	-0.9	-1.2	-1.8	-1.3	1.3	2.5
330	-0.9	-1.1	-1.8	-1.3	1.3	2.6
340	-0.8	-1.0	-1.7	-1.2	1.3	2.6
350	-0.5	-0.2	-1.3	-0.7	1.6	3.3

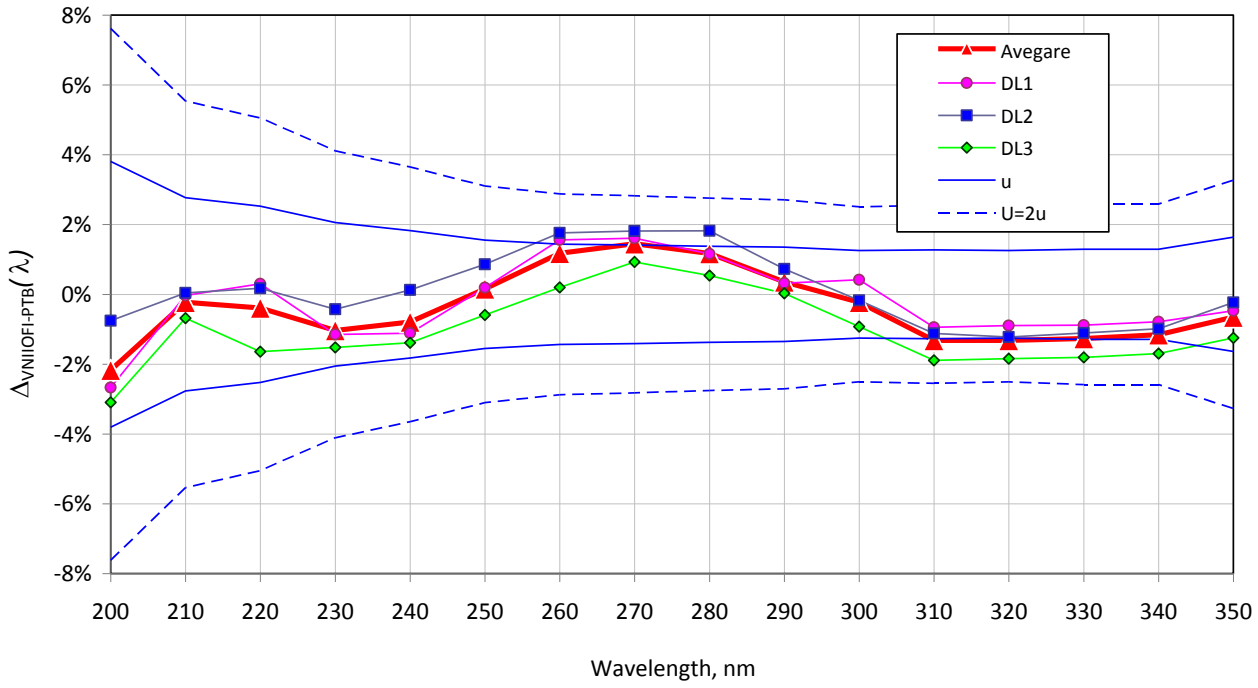

Figure 9.1. VNIIOFI to PTB differences for individual lamps (Eq. 9.1) and average (Eq. 9.4). The blue solid line and blew dashed line indicate the standard (Eq. 9.5) and expanded (Eq. 9.6), respectivaly.

9.2 VNIIOFI Degree of Equivalence

Unilateral degree of Equivalence (DoE) of VNIIOFI $D_{\mathrm{VNIIOFI}}(\lambda)$ was calculated in accordance with the analysis method A2.1 of CCPR-G6:

$$D_{\mathrm{VNIIOFI}}(\lambda) = D_{\mathrm{PTB}}(\lambda) + \left(E_{\lambda,\mathrm{VNIIOFI}}(\lambda)/E_{\lambda,\mathrm{PTB}}(\lambda) - 1\right) = D_{\mathrm{PTB}} + \Delta_{\mathrm{VNIIOFI-PTB}}(\lambda) \tag{9.7}$$

where $D_{\mathrm{PTB}}(\lambda)$ is the unilateral DoE of PTB.

Table 9.2. PTB unilateral DoEs $D_{\mathrm{PTB}}(\lambda)$ and their expanded uncertainties $U(D_{\mathrm{PTB}})$, and random effects uncertainty $u_{PTB,r,RMO}$

λ Wavelength nm	$D_{\mathrm{PTB}}(\lambda)$ %	$U(D_{\mathrm{PTB}})$ %	$u_{PTB,r,RMO}$ %
200	0.8	3.9	1.5
210	1.8	2.9	0.9
220	1.1	2.7	0.9
230	1.0	2.1	0.5
240	0.4	2.1	0.5
250	0.2	1.6	0.3
260	0.1	1.6	0.3
270	-0.2	1.8	0.4
280	-0.4	1.9	0.4
290	-0.5	2.0	0.5
300	-0.9	1.9	0.5
310	-1.2	2.2	0.6
320	-1.2	2.1	0.6
330	-0.5	2.5	0.7
340	-1.0	2.5	0.7
350	-1.8	3.6	1.3

The uncertainty of the unilateral DoE of VNIIOFI is given as an expanded uncertainty

$$U(D_{\mathrm{VNIIOFI}}) = 2 \cdot u(D_{\mathrm{VNIIOFI}}) \tag{9.8}$$

where the standard uncertainty was calculated as (see the equation 6 of CCPR-G6):

$$u^2(D_{\mathrm{VNIIOFI}}) = \left(\frac{U(D_{\mathrm{PTB}})}{2}\right)^2 + u^2_{\mathrm{VNIIOFI}} + u^2_{PTB,r,RMO} \tag{9.9}$$

where:

$U(D_{\mathrm{PTB}})$ is the expanded uncertainty of unilateral DoE of PTB. The values of PTB unilateral DoEs $D_{\mathrm{PTB}}(\lambda)$ and corresponding expanded uncertainty $U(D_{\mathrm{PTB}})$ are published in the CCPR-K1b final report, Table 10.2 [1], and, for convenience, presented in Table 9.2 of this document.

u_{VNIIOFI} is standard uncertainty of VNIIOFI measurements, presented in Table 4.6.

$u_{PTB,r,RMO}$ is the standard uncertainty associated with uncorrelated (random) effects of the link laboratory (PTB) during the RMO comparison. This uncertainty is a combination (square root of the sum of squares) of the following components of the PTB uncertainty budget presented in Table 5.3: "stability of facility and monitor lamp", "standard deviation of working standard", "standard deviation of transfer standard" and "reproducibility of transfer standard". The values of $u_{PTB,r,RMO}$ are presented in Table 9.2.

The VNIIOFI unilateral DoEs and their uncertainties are presented in Table 9.3

Table 9.3. VNIIOFI unilateral DoEs $D_{\mathrm{VNIIOFI}}(\lambda)$ and their standard $u(D_{\mathrm{VNIIOFI}})$ and expanded $U(D_{\mathrm{VNIIOFI}})$ uncertainties

λ Wavelength nm	$D_{\mathrm{VNIIOFI}}(\lambda)$ %	$u(D_{\mathrm{VNIIOFI}})$ %	$U(D_{\mathrm{VNIIOFI}})$ %
200	-1.4	5.4	10.8
210	1.6	4.0	8.0
220	0.7	3.6	7.2
230	0.0	2.9	5.8
240	-0.4	2.7	5.4
250	0.4	2.2	4.4
260	1.3	2.1	4.2
270	1.2	2.2	4.4
280	0.8	2.3	4.6
290	-0.1	2.4	4.8
300	-1.1	2.3	4.6
310	-2.5	2.5	5.0
320	-2.5	2.4	4.8
330	-1.8	2.8	5.6
340	-2.2	2.8	5.6
350	-2.5	4.0	8.0

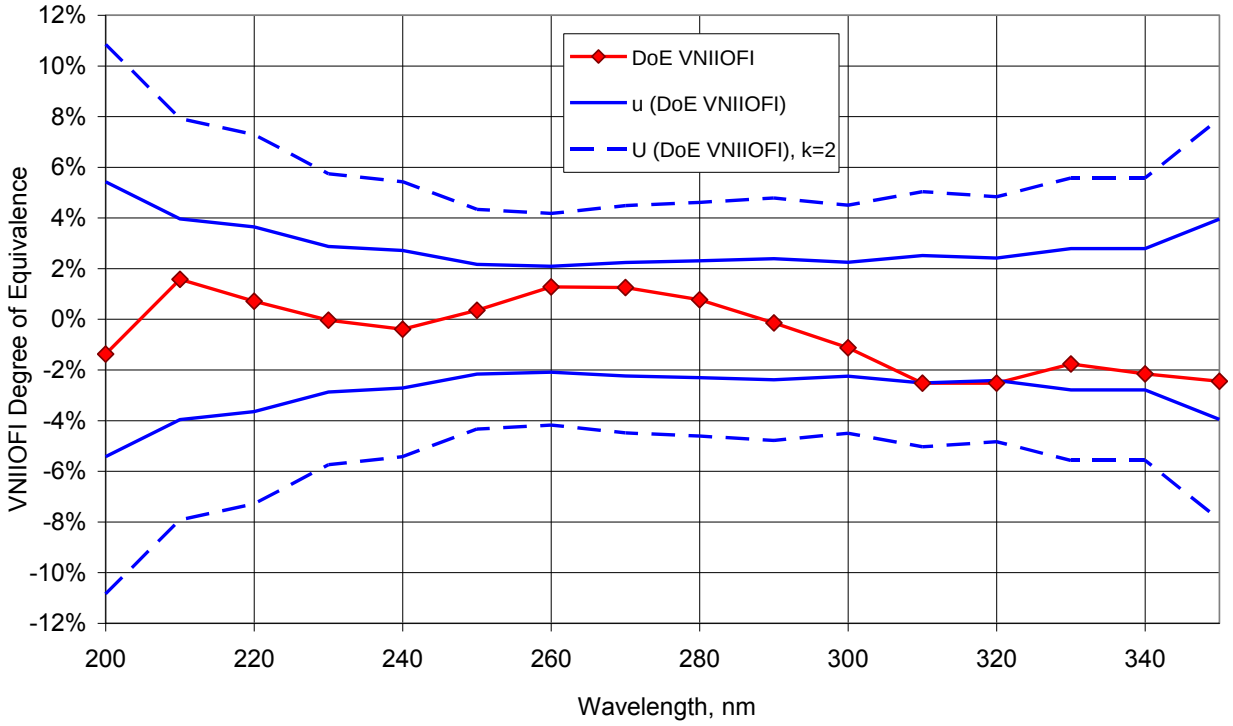

Figure 9.2. VNIIOFI unilateral DoEs and their standard and expanded (*k*=2) uncertainties

References

[1] P. Sperfeld, Final report on the CIPM key comparison CCPR-K1.b: Spectral irradiance 200 nm to 350 nm, *Metrologia*, 2008, **45**, *Tech. Suppl.*, 02002, doi:10.1088/0026-1394/45/1A/02002. (http://iopscience.iop.org/article/10.1088/0026-1394/45/1A/02002/meta)

[2] Guidelines for CCPR and RMO Bilateral Key Comparisons, CCPR-G5 (http://www.bipm.org/en/committees/cc/ccpr/publications-cc.html)

[3] Guidelines for RMO PR Key Comparisons, CCPR-G6 (http://www.bipm.org/en/committees/cc/ccpr/publications-cc.html)

[4] Guidelines for CCPR Key Comparison Report Preparation, CCPR-G2 (http://www.bipm.org/en/committees/cc/ccpr/publications-cc.html)

[5] Birch K. P. and Downs M. J., Correction to the updated Edlén equation for the refractive index of air, *Metrologia*, 1994, **31**, 315–316 (http://www.kayelaby.npl.co.uk/general_physics/2_5/2_5_7.html)

[6] E. R. Woolliams et. al., Thermodynamic temperature assignment to the point of inflection of the melting curve of high-temperature fixed points, *Phil.Trans.R.Soc.A* **374**: 20150044

[7] B. B. Khlevnoy and I. A. Grigoryeva, Long-Term Stability of WC-C Peritectic Fixed Point, *Int J Thermophys* (2015) **36**:367–373

[8] http://www.virial.com/steep321.html

[9] P. Sperfeld, S. Pape, B. Khlevnoy and A. Burdakin, Performance limitations of carbon-cavity blackbodies due to absorption bands at the highest temperatures, *Metrologia*, **46** (2009) S170–S173

[10] Metzdorf J., Metrologia, 1993, 30, 403-408.

[11] Sapritsky V. I., Khlevnoy B. B., Khromchenko V. B., Lisiansky B. E., Mekhontsev S. N., Melenevsky U. A., Morozova S. P., Prokhorov A. V., Samoilov L. N., Shapoval V. I., Sudarev K. A., Zelener M. F., Appl. Opt., 1997, 36, 5403-5408.

[12] Sperfeld P., Metzdorf J., Galal Yousef S., Stock K. D., Möller W., Metrologia, 1998, 35, 267-271. [4]

[13] Sperfeld P., Metzdorf J., Harrison N. J., Fox N. P., Khlevnoy B. B., Khromchenko V. B., Mekhontsev S. N., Shapoval V. I., Zelener M. F., Sapritsky V. I., Metrologia, 1998, 35, 419-422.

[14] Sperfeld P., Entwicklung einer empfängergestützten spektralen Bestrahlungs-stärkeskala, Braunschweig, 1999. http://www.biblio.tu-bs.de/ediss/data/19990628a/19990628a.html

[15] Khlevnoy B.B., Harrison N.J., Rogers L.J., Pollard D.F., Fox N.P., Sperfeld P., Fischer J., Friedrich R., Metzdorf J., Seidel J., Samoylov M.L., Stolyarevskaya R.I.,

[16] Khromchenko V.B., Ogarev S.A., Sapritsky V.I., Metrologia, 2003, 40, S39–S44

[17] Cox M.G., Harris P.M., Kenward P.D., Woolliams E.R., "Spectral characteristic modelling", NPL Report CMSC 27/03. Available at: http://www.npl.co.uk/ssfm/download/